

Oak Ridge National Laboratory GMLC 1.4.9 Technical Report: Data Analytics for Electrical Distribution Systems with Micro PMUs



Raymond C Borges Hink
Emilio C Piesciorovsky

July 2019

Approved for public release.
Distribution is unlimited.

DOCUMENT AVAILABILITY

Reports produced after January 1, 1996, are generally available free via US Department of Energy (DOE) SciTech Connect.

Website www.osti.gov

Reports produced before January 1, 1996, may be purchased by members of the public from the following source:

National Technical Information Service
5285 Port Royal Road
Springfield, VA 22161
Telephone 703-605-6000 (1-800-553-6847)
TDD 703-487-4639
Fax 703-605-6900
E-mail info@ntis.gov
Website <http://classic.ntis.gov/>

Reports are available to DOE employees, DOE contractors, Energy Technology Data Exchange representatives, and International Nuclear Information System representatives from the following source:

Office of Scientific and Technical Information
PO Box 62
Oak Ridge, TN 37831
Telephone 865-576-8401
Fax 865-576-5728
E-mail reports@osti.gov
Website <http://www.osti.gov/contact.html>

This report was prepared as an account of work sponsored by an agency of the United States Government. Neither the United States Government nor any agency thereof, nor any of their employees, makes any warranty, express or implied, or assumes any legal liability or responsibility for the accuracy, completeness, or usefulness of any information, apparatus, product, or process disclosed, or represents that its use would not infringe privately owned rights. Reference herein to any specific commercial product, process, or service by trade name, trademark, manufacturer, or otherwise, does not necessarily constitute or imply its endorsement, recommendation, or favoring by the United States Government or any agency thereof. The views and opinions of authors expressed herein do not necessarily state or reflect those of the United States Government or any agency thereof.

Electrical and Electronics Systems Research Division

**GMLC 1.4.9 Technical Report:
Data Analytics for Electrical Distribution Systems with Micro PMUs**

Raymond C Borges Hink
Emilio C Piesciorovsky

July 2019

Prepared by
OAK RIDGE NATIONAL LABORATORY
Oak Ridge, TN 37831-6283
managed by
UT-BATTELLE, LLC
for the
US DEPARTMENT OF ENERGY
under contract DE-AC05-00OR22725

CONTENTS

CONTENTS	iii
LIST OF TABLES	iii
LIST OF FIGURES	iv
ACRONYMS	v
excutive summary	1
1. INTRODUCTION	3
2. LITERATURE REVIEW	4
2.1 DATA ANALYTICS FOR ELECTRICAL DISTRIBUTION UTILITTIES AND CUSTOMERS	4
2.2 EMERGING CHALLENGES IN ANALYTICS FOR ELECTRICAL DISTRIBUTION	6
3. TECHNICAL APPROACH	7
3.1 TESTBED	7
3.2 SYNCHROPHASOR SYSTEM	9
3.3 SETTINGS OF MICRO PMUS	11
3.4 SETTING OF PHASOR DATA CONCENTRATOR	14
3.5 MONITORING THE MICRO PMUS	19
4. DATASETS AND EXPERIMENTS	24
4.1 AVAILABLE MICRO PMU DATA FOR ANALYTICS	26
4.2 OPENFMB DATA	27
4.3 PCAP DATA	28
5. RESULTS	28
5.1 TEST AND COLLECTED DATA FOR ANALYTICS	28
5.1.1 Data from the “ORNL_PMU01” micro PMU	29
5.1.2 Data from the “ORNL_PMU02” micro PMU	32
6. DISCUSSIONS	35
6.1 SAMPLE RATE & DATA ANALYTICS	35
6.2 DATA ANALYTICS MAP FOR BREAKER OPERATION TESTS WITH MICRO PMUS	38
6.3 COMPARISON OF OPENFMB AND LBNL STREAM-PROCESSING ARCHITECTURE FOR REAL-TIME CYBERPHYSICAL SECURITY (SPARCS)	40
7. CONCLUSIONS	41
REFERENCES	42

LIST OF TABLES

Table 1: Data analytics for electrical distribution utilities and customers	5
Table 2: List of synchrophasor software	10
Table 3: Communication parameters to collect binary data from the micro PMUs	22
Table 4: Description of experiment datasets	24
Table 5: Data analytics estimated by the micro PMUs	26
Table 6: Map of available data analytics for breaker operation tests with micro PMUs	39
Table 7: Comparison of SPARCS and OpenFMB	40

LIST OF FIGURES

Figure 1: Diagram of electrical distribution utility and customers	5
Figure 2: Micro PMU Data analytics testbed.....	7
Figure 3: Framework for system and communication architecture	9
Figure 4: Configuration of the primary and secondary frameworks.....	10
Figure 5: Software steps for the implementation of the Synchrophasor system.....	11
Figure 6: PQube general info setting for “PMU_01” micro PMU	11
Figure 7: AC voltage (A) and current (B) ratio settings for the micro PMUs.....	12
Figure 8: Network settings for the “PMU_01” micro PMU	12
Figure 9: Security settings for the micro PMUs	13
Figure 10: micro PMU (A) and C37 communication (B) settings for the “PMU_01” micro PMU.....	13
Figure 11: Steps to download and send the “Setup.ini” file to the micro PMU	14
Figure 12: Communication parameters (A-B) and micro PMU connection steps (C).....	15
Figure 13: Steps to save the Connection (A) and Configuration (B) files.....	16
Figure 14: Steps to open the “Input Device Wizard”	16
Figure 15: Launch Walkthrough to set the Connection file.....	17
Figure 16: Launch Walkthrough to set the Configuration file.....	18
Figure 17: Steps to enable the data stream of micro PMUs.....	19
Figure 18: Steps to plot the stream data from micro PMUs.....	20
Figure 19: Steps to find the Description of Signal References for the micro PMUs.....	21
Figure 20: Steps to communicate with micro PMUs by the FileZilla Client® [21] software	21
Figure 21: Steps to download the binary data files from the micro PMUs.....	22
Figure 22: Steps to convert “binary.dat” into an “Excel” file for micro PMUs	23
Figure 23: Impact on Modbus traffic based on data IO in packets per 100ms for each experiment	25
Figure 24: UDP packet flood effect on breaker 1 Modbus network responsiveness.....	25
Figure 25: Circuit and sequence for breaker operation tests.....	28
Figure 26: Initial and final test times from the “ORN_PMU01” and “ORNL_PMU02” micro PMUs	29
Figure 27: L1 current RMS fundamental magnitude (A) and angle (C), and L1-E voltage RMS fundamental magnitude (B) and angle (D) from the “ORNL_PMU01” micro PMU.....	31
Figure 28: Fundamental apparent, true and reactive total power (A), total displacement power factor (B) from the “ORNL_PMU01” micro PMU	31
Figure 29: Fundamental apparent and, true total power (A), and zoom in total displacement power factor (B) from the “ORNL_PMU01” micro PMU	32
Figure 30: C37 and one-second Frequency from the “ORNL_PMU01” micro PMU.....	32
Figure 31: L1 current RMS fundamental magnitude (A) and angle (B) from the “ORNL_PMU02” micro PMU.....	33
Figure 32: L1 current (A) and L1-E voltage (B) fundamental angles from the “ORNL_PMU02” micro PMU.....	34
Figure 33: Fundamental apparent, true and reactive total power (A), and total displacement power factor (B) from the “ORNL_PMU02” micro PMU	35
Figure 34: C37 and one-second Frequency from the “ORNL_PMU02” micro PMU.....	35
Figure 35: Setting screen of sample rate for the micro PMU	36
Figure 36: Sample rate curves for PMU, Relay, and micro PMU	37
Figure 37: Nyquist frequency for PMU, Relay, and micro PMU	37

ACRONYMS

OpenFMB	Open Field-Message-Bus
PMUs	Phasor Measurement Units
IEDs	Intelligent Electronic Devices
DA	Data Analytics
kWh	kilo Watt hour
kVARh	kilo Volt Ampere Reactive hour
CO ₂	Carbon Dioxide
U.S.	United States
SCADA	Supervisory Control and Data Acquisition
PDC	Phasor Data Concentrator
GPS	Global Positioning System
NI	National Instruments
sbRIO	single board RIO
GPIC	General Purpose Inverter Controller
Modbus TCP	Modbus Transmission Control Protocol
X/R	Reactance / Resistance
NATS	Open-Source Messaging System
PA	Process Automation
SEL	Schweitzer Engineering Laboratories
IEEE	Institute of Electrical and Electronics Engineers
ORNL	Oak Ridge National Laboratory
BK	Breaker
UTC	Coordinated Universal Time
FTP	File Transfer Protocol
AC	Alternative Current
RMS	Root Mean Square
IP	Internet Protocol
TCP	Transmission Control Protocol
W	Fundamental Total True Power
VAR	Fundamental Total Reactive Power
VA	Fundamental Total Apparent Power
dPF	Fundamental Total Displacement Power Factor
ADC	Analog Digital Converter
SR	Sample Rate
PWM	Pulse Width Modulation
AC/DC	Alternative Current / Direct Current

EXECUTIVE SUMMARY

This report describes how electrical utilities with residential, industrial, commercial and government customers make decisions using Data Analytics (DA) applications and discusses how OpenFMB was leveraged to share that data among disparate types of devices for DA. OpenFMB is a data standard developed by utilities for distributed communication and control of power system assets [13]. We explore how OpenFMB can be used for sharing analytics and what those analytics could be for a set of representative grid devices. We present a review of DA applications performed by electrical utilities and customers. An overview of how the testbed we used was configured is summarized. Several experiments which were carried out to explore the capabilities of OpenFMB alongside other data sharing mechanisms for gathering sensor measurements and sharing analytics is also discussed. And finally, a comparison of OpenFMB and LBNL's SPARK framework is summarized.

Today's PMUs and Relays can measure voltage and current signals of 60 and 48 harmonics, respectively. PMUs and Relays can allow the estimation for normal operation (oscillating at 60 Hz), and harmonics disturbances in power systems. However, micro PMUs allow 120 samples per second, and they should be used for normal operation (oscillating at 60 Hz) in power systems. In addition, most DA applications applied currently by electrical utilities focus on residential, industrial, commercial and government customers, while transportation customers (electrical cars, vans, trucks, buses, subway, rail, and trolley systems) represent less than 1% of total U.S. electricity. The growing demand of electrical vehicles could require studying the impact of transportation customers in the near future, to know what and how DA applications will be applied between electrical utilities and transportation customers.

Electrical utilities focus on monitoring the real-time customer consumptions, offering new real-time tariff models based on customer usage habits (rewards and punishments), providing energy peak during peak load times (plan energy generation and distribution), improving the load management for transformers and power lines, and controlling the energy and grid resources efficiently. On the other hand, the DA applications for residential customers are based on modifying the customer electricity usage habit to save money, making accurate and timely decisions for electrical billing. However, the DA applications for industrial, commercial and government customers focus on creating efficient programs to improve the environmental condition (reducing CO2 emission), developing better load forecasting for industrial and/or commercial activities.

In this project we configured a testbed to explore how the OpenFMB framework can be used to distribute data among various types of representative grid edge devices. We used Micro PMUs (Phasor Measurement Unit) to collect and transmit data from relays to an OpenPDC server. We also configured OpenFMB framework to collect and transmit data from various relays. The testbed was composed of a physical asset based on a 60 Hz AC radial power system constructed using SI-GRID components [34]. The power system consisted of a 3-phase 14 volts line-to-ground (24 volts line-to-line) power source, three 3-phase line emulators, a programmable resistive load bank, two smart relays, two micro PMUs, and a supervisory control and data acquisition (SCADA) system and Phasor Data Concentrator (PDC) computer.

This testbed configuration allowed us to perform breaker operations and collect data from the micro PMUs and from the relays' sensors. During the micro PMU breaker operation tests, we collected the measured and estimated fundamental voltages, currents, frequency as well as the total true, reactive and apparent power. The displacement power factor from two micro PMUs located in parallel power lines was also used. The software steps for the implementation of the Synchrophasor system are explained in detail in this report. The setting and data collection phases were performed with open source software. In the setting phase, the micro PMUs were set, the data stream for each micro PMU was validated, and the

connection and configuration files were created. The PDC computer was set using the connection and configuration files of the micro PMUs. In the data collection phase we induced simple events like relays opening and closing and collected the binary data from the micro PMUs. Then we converted the binary data files of the micro PMUs to analyze the test results. We configured OpenFMB to use protocol translators to read Modbus and transform the reading into the OpenFMB data model to be read for DA applications.

Our experiments explored how leveraging the OpenFMB data model and micro PMUs together we can obtain a varied view of network faults via redundant data sources. In some cases where network faults lead to failures in the system corroborating these observed phenomenon with redundant data sources helped validate the observation. For example, in one experiment the fundamental RMS current angle, and the fundamental displacement power factor (estimated by the ratio between the measured real and apparent total power) suffered a disturbance at the micro PMU connected to the beginning of the parallel power line which we were able to validate by matching up the data pattern with the redundant data sources.

Based on the breaker state scenarios and micro PMU locations, the DA applications using the current angle and displacement power factor from the micro PMUs should be studied in detail to avoid a non-desired measurement that could affect the decision from the DA. Also, the sample rates for PMU, Relay and micro PMU devices were compared. The higher the sample rate, the better the quality of the measurement for DA estimations.

1. INTRODUCTION

The growing implementation of smart grid applications requires electrical utilities to integrate control activities with DA implementations to improve their operation [1]. The authors in [2] suggest Electrical utilities increase inter-operability among intelligent electronic devices (IEDs) and systems to advance grid operation and control efficiency. Data analytics is the process of examining data sets in order to draw conclusions about the information they contain [3]. The implementation of DA is applied between electrical utilities and customers (residential, industrial, commercial and government) by collecting data, and making decisions [2]. Electrical utilities at transmission areas have used the state of voltage vectors of power lines and their physical behavior is well-understood [4]. On the other hand, distribution system operators have not had a detailed real-time actionable information about the electrical grid at the distribution level [5].

The electrical measurements collected from the utility's customers along the grid can also provide information to make decisions. The visualization and interpretation of raw sensor streams can be enormous, and it can be a difficult task for distribution system operators, considering the large quantity of data [6]. Then, it is crucial to mine the collected data with analytic tools that can generate informative measurements and automated reports, to be used by electrical utilities and customers. Recent literature reviews focuses on the PMU data utilization at the transmission level to improve wide-area monitoring, protection, and control [7, 8], however, distribution grids are still lagging behind in that respect, since tools for the transmission grid may not be directly applicable to the distribution grid.

As distribution grids are converting from a demand-serving network towards an interactive grid, there is a growing interest in gaining situational awareness via advanced sensors such as micro PMUs [9]. The deployment of the micro PMUs in isolation without additional data driven applications and analytics are insufficient. Therefore, it is important to equip distribution system operators with complimentary software tools capable of mining these large data sets in search of useful information and a data model that can adequately share data among different types of devices.

In this work, we describe how electrical utilities with residential, industrial, commercial and government customers make decisions using DA applications. Today's electrical utilities focus on monitoring the real-time customer's consumptions, offering new real-time tariff models based on customer usage habits (rewards and punishments), providing energy peak during peak load times (plan energy generation and distribution), improving the load management for transformers and power lines, and controlling the energy and grid resources efficiently. On the other hand, the DA applications for residential customers are based on modifying the customer electricity usage habit to save money, making accurate and timely decisions for electrical billing. However, the DA applications for industrial, commercial and government customers focus on creating efficiency programs to improve the environmental condition (reducing CO2 emission), developing better load forecasting for industrial and/or commercial activities.

We configured our micro PMU DA testbed to collect data with a SCADA leveraging OpenFMB and a Synchrophasor system. We recorded breaker operation tests by collecting data from the micro PMUs sensors. During the micro PMU breaker operation tests, the fundamental voltages, currents, frequency, and total true, reactive and apparent power, and displacement power factor were collected from two micro PMUs located at parallel power line.

The steps for implementation of the Synchrophasor system are explained in detail. Based on the breaker state scenarios and micro PMU locations, the data collected from the micro PMUs were studied to observe their behavior for DA applications. The sample rates for PMU, Relay and micro PMU devices

were compared. The higher the sample rate, the better the quality of the measurement for DA estimations. The sample rates for PMU, Relay and micro PMU devices were compared to study the impact of collected data from measurement devices at DA applications for power systems at normal (oscillating at 60 Hz) and non-normal (disturbances with harmonics components) operations.

2. LITERATURE REVIEW

2.1 DATA ANALYTICS FOR ELECTRICAL DISTRIBUTION UTILITIES AND CUSTOMERS

Today's electrical distribution utilities have increased the inter-operability among customers because of the great number of protective relays, PMUs, and smart meters installed along the electrical grid [10]. These devices can be used to perform DA, draw conclusions and make decisions to improve the utility-grid-customer operation and control efficiency. The implementation of DA could be applied by electrical utilities to residential, industrial, commercial and government customers. The residential customers include single-family homes and multi-family housing, and they represent more than one third of the electricity used nationwide. The largest use of electricity by residential customers is air conditioning, lighting, water heating, space heating, and appliances.

The electricity demand in the residential sector tends to be highest on hot summer afternoons due to increased air conditioning use, followed by evenings, when lights are turned on [11]. The commercial and government customers are service-providing facilities, and other public and private organizations. The commercial customers represent more than one third of U.S. electricity consumption. The largest use of electricity by commercial customers is lighting and heating, ventilation, and air conditioning. The electricity demand in the commercial sector tends to be highest during operating business hours, and it decreases substantially on nights and weekends [11]. The industrial customers are represented by facilities that use electricity for processing, producing, or assembling goods (manufacturing, mining, agriculture, and construction industries). The industrial customers use less than one third of the nation's electricity. The manufacturing facilities use more than half of the electricity for powering motors (machine drives).

Other sizable uses include heating, cooling, and electro-chemical processes in which electricity is used to cause a chemical transformation (steel, aluminum and petrochemical plants). The electricity in the industrial sector tends to not fluctuate throughout the day or year, as opposed to residential and commercial sectors [11]. The transportation customers are vehicles that use electricity from the electric power grid. The transportation customers include electrical cars, vans, trucks, buses, subway, rail, and trolley systems. The transportation customers account for less than 1% of the total U.S. electricity. However, this electricity consumption could grow as electric vehicles become more common in the near future [11]. The diagram of electrical distribution utility and customers is shown in Figure 1.

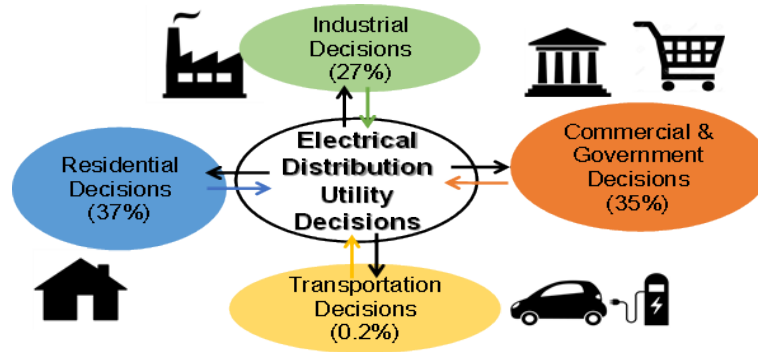


Figure 1: Diagram of electrical distribution utility and customers

To allow utilities to make more efficient use of the energy and grid resources it is crucial for electrical distribution utilities and different customers to be able to take advantage of sharing the DA. On the other hand, residential customers could save money in their electrical bills, industrial plants could decrease the environmental impact by reducing CO₂ emission, and government buildings can lead energy efficient programs by acquiring knowledge of the consumption pattern. Table 1 shows traditional DA that could be applied by electrical distribution utilities and their residential, industrial, commercial and government customers.

Table 1: Data analytics for electrical distribution utilities and customers

<i>Utility</i>	<i>Customers</i>				
	<i>Residential</i>		<i>Industrial, Commercial & Government</i>		
Data	Decisions	Data ^[a]	Decisions	Data	Decisions
kWh, kVARh, power factor	To monitor real-time customer consumptions	kWh/month	To modify customer electricity usage habit to save money	kWh/month	To create efficiency programs to decrease the environmental impact (reducing CO ₂ emission)
kWh, kVARh, power factor	To offer new real-time tariff models based on customer usage habits (rewards and punishments)	kWh/day	To make accurate and timely decisions for electrical billing	kWh/day	To create better load forecasting for industrial and/or commercial activities
Peak loads	To provide energy peak during peak load times (plan energy generation and distribution)	Voltage and Frequency	To supervise energy quality provided by the utility to avoid damage to electrical appliances	Voltage and Frequency	To supervise energy quality provided by the utility to avoid damage to electrical industrial equipment
Line and Transformer power losses	To improve the transformer load management for the power lines	On-peak times	To operate electrical equipment during hours with less expensive fees	On-peak times	To operate electrical equipment during hours with less expensive fees

Voltage, Frequency, Active Power, Reactive Power	To control energy and grid resources efficiently	Programmed energy blackouts	To program home tasks and turn-off sensitive electrical equipment that could be damaged during blackout	Power Factor	To install capacitor banks to avoid utility's bill penalties
Main Breaker States	To define actual grid modes and possible grid operations	Programmed energy restorations	To program home tasks and turn-off sensitive electrical equipment that could be damaged during blackout	Programmed energy blackouts / restorations	To program gen-backup plans for industrial and/or commercial activities

^[a] Data sent by utilities to customers through apps installed in customer's cellphones

2.2 EMERGING CHALLENGES IN ANALYTICS FOR ELECTRICAL DISTRIBUTION

One of the biggest emerging challenges in the electrical grid is managing and analyzing big data. Because of the increasing number of measurement devices that generate massive amounts of time-series data and other types of sensor types that also generate data, the electric grid operator needs new data system architectures that can collect and effectively transform the data collected into useful meaningful information and knowledge. Some of the challenges with data in the next generation power grid include [29]:

- Unstructured data – tools like NoSQL databases are starting to catch on to solve this issue
- High volumes of data – the increasing number of sensors and granularity of measurements
- Diversity and heterogeneity – the various formats of data and different types of devices collecting the data.
- Timeliness and quality – measuring latency, error rates, and data loss may increase system risk and operation cost
- Computation burden - larger amounts of data may need to be analyzed for decision making within a very short time, supercomputing with GPUs may be integrated as edge devices

Data analytics also create significant savings from predictive maintenance. By predicting transformer failures before they occur some utilities have reportedly saved millions [30]. OpenFMB adds to these savings by generalizing data formatting for analytic flexibility. Increasing amounts of system integration are layered and analyzed by artificial intelligence (AI) with machine learning and therefore common communication protocol standards that can unify the data model for the various systems and AI applications such as OpenFMB tie in well here.

Challenges that we hope to address in future work include: a) addressing discarded data, b) addressing siloed data, c) supporting real-time analytics, d) coexistence of centralized and decentralized data management, e) balancing integrated and disintegrated systems and f) customizing data management systems for speed and versatility. It is also important to note that privacy and security play a big role in all of this and security solutions will need to conform to the new data architecture [31].

3. TECHNICAL APPROACH

3.1 TESTBED

The micro PMU DA testbed to collect data at distribution power system consisted of a primary and secondary framework serving as two types of side-by-side data aggregation protocols. Open Field-Message-Bus (OpenFMB) was used as the primary framework and synchrophasor systems were used as a secondary framework respectively. In this study, a physical asset based on a 60 Hz AC radial power system was used, which was constructed by using SI-GRID components. The system consisted of a 3-phase 14-volt line-to-ground (24 volts line-to-line) power source, three 3-phase line emulators, a controllable resistive load bank, two smart relays, two micro phasor measurement units (PMUs), and a Supervisory Control and Data Acquisition (SCADA) and Phasor Data Concentrator (PDC) computers. Figure 2 shows the testbed.

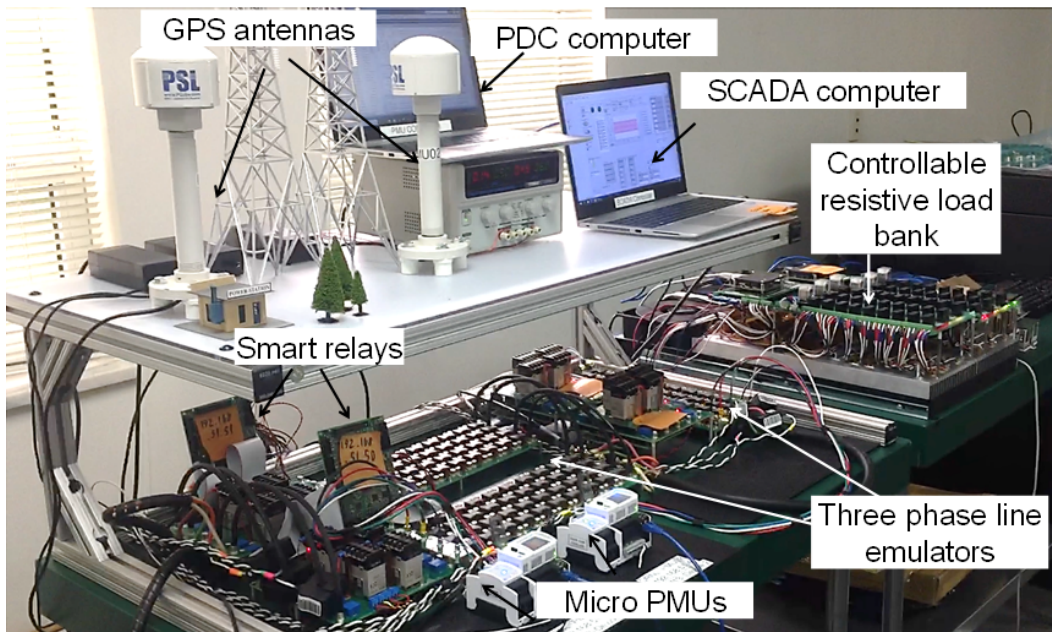


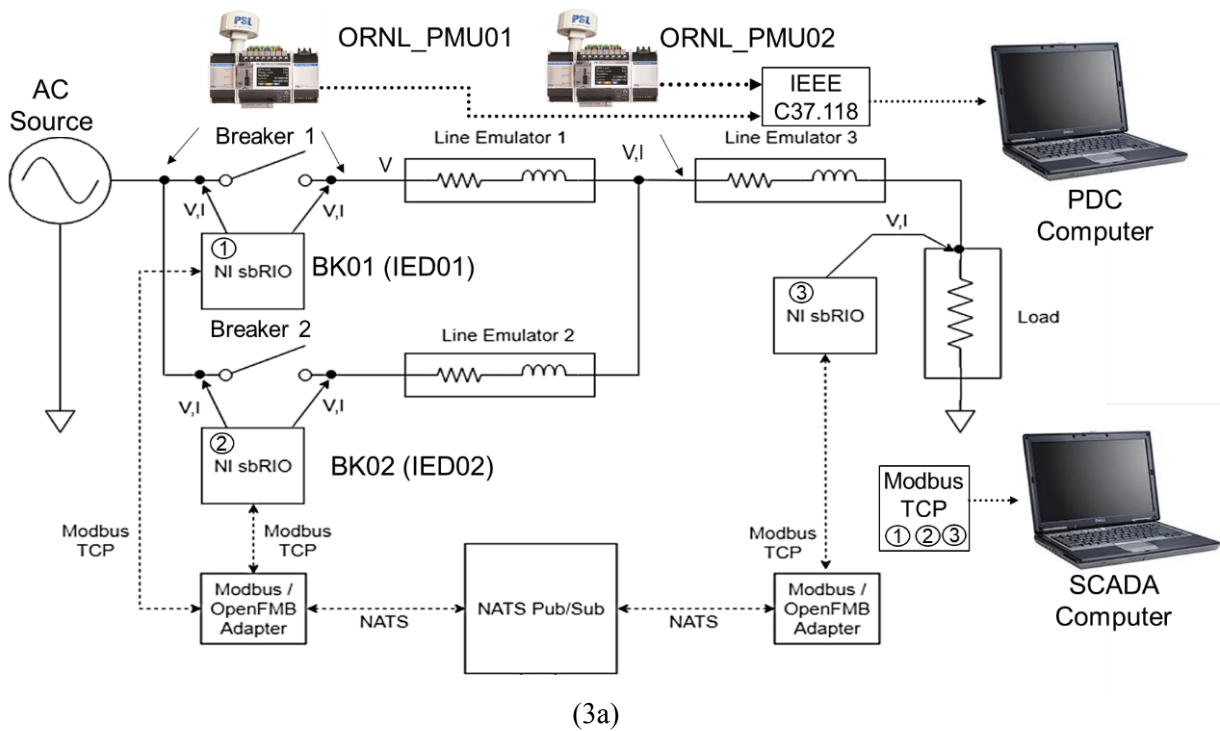
Figure 2: Micro PMU Data analytics testbed

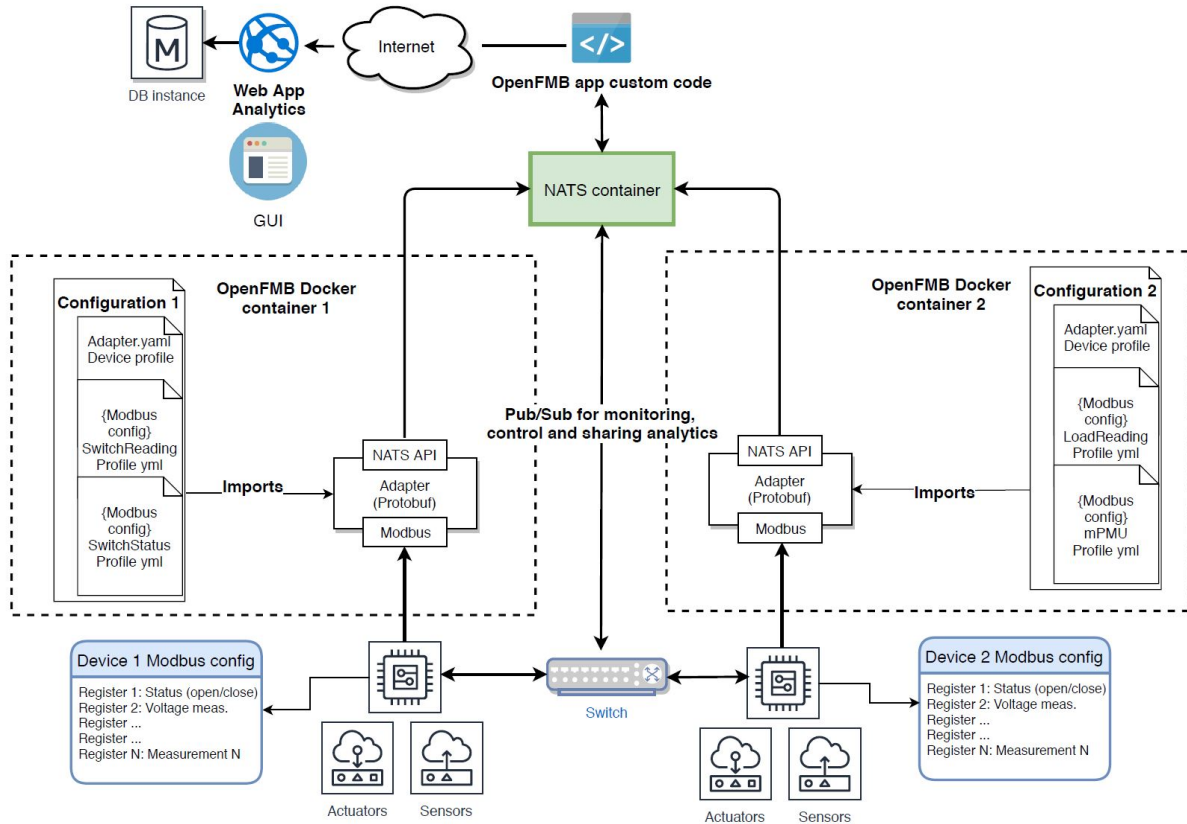
In the micro PMU DA testbed, a National Instruments (NI) single board RIO (sbRIO) provided the control and data acquisition for the load bank. Each load bank has a maximum load of 300 watt per phase at 24 volts line-to-line voltage, and it is controllable to within 1 watt. The sbRIO connects directly to the relaying and measurement board through a General Purpose Inverter Controller (GPIC) [12]. This provides high-sample-rate of voltage and current measurements at the load. The load bank also supports individual phase control for testing of unbalanced systems and unbalanced load profile playback. The control and monitoring interface used for the load bank was Modbus Transfer Control Protocol (TCP). Similarly, the control and instrumentation switches were provided by an NI sbRIO. The sbRIO provided highly sampled voltage and current readings on both sides of the breaker, as well as local and remote control of the breaker state (open/close).

Like the load bank, the control and monitoring interface was controlled using Modbus TCP. The three 3-phase, 5-wire line emulators adds resistive and inductive impedance to the system. Each line emulator had ten series inductors per phase, totaling 220 μH at an X/R ratio of approximately eight. Each line emulator represents approximately 1,000ft of medium-voltage distribution line. A NATS pub/sub system

with an OpenFMB data model provided data acquisition and control for the system and from the relay sensors as well as the programmable load bank sensors.

Translators polled Modbus data from different assets, loaded the data into the appropriate OpenFMB data structures, and published the OpenFMB data over the NATS pub/sub protocol. Similarly, translators subscribed to relevant OpenFMB commands on the NATS network and translated them into appropriate Modbus commands for the devices. The testbed in Figure 2 was also connected to a SEL 3360 compact industrial computer. The OpenFMB translators were built into Docker [14] containers that were hosted on the SEL 3360 compact industrial computer running in Linux. On the other hand, the secondary framework with the micro PMUs were connected to a PDC computer by using IEEE C37.118-2011 synchrophasor protocol. An overview of the overall system and communication architecture is shown in Figure 3a. Figure 3b shows a potential architecture for use with a backend web-based analytics interface.





(3b)

Figure 3: Framework for system and communication architecture

3.2 SYNCHROPHASOR SYSTEM

The Synchrophasor system was the secondary framework for the SCADA and OpenFMB systems. Initially the plan was to join the OpenFMB system with the synchrophasors but there were no compatible OpenFMB protocol translators for the C37.118-2011 (C37) protocol to the OpenFMB data model and our solution to use an RTAC as a Modbus to C37.118-2011 protocol translator did not work. C37.118-2011 is also much faster than Modbus and therefore we opted to implement the micro PMUs as a secondary or backup framework to the main system and leverage them to study what type of analytics could be suggested to the OpenFMB working group for future implementation in a data analytics profile instead.

In the testbed, the controllable resistive load bank was energized by two breakers named as “BK01” and “BK02”. The synchrophasor system was implemented by installing two micro PMUs named as “ORNL_PMU01” and “ORNL_PMU02”. These micro PMUs were located at buses of power lines in the testbed. The Synchrophasor and SCADA systems were implemented by the IEEE C37.118-2011 and Modbus protocols, respectively. The SCADA computer collected the voltages, currents and states of the breakers. The PDC computer collected the data from the micro PMUs. The configuration of the primary and secondary frameworks for the testbed is shown in Figure 4.

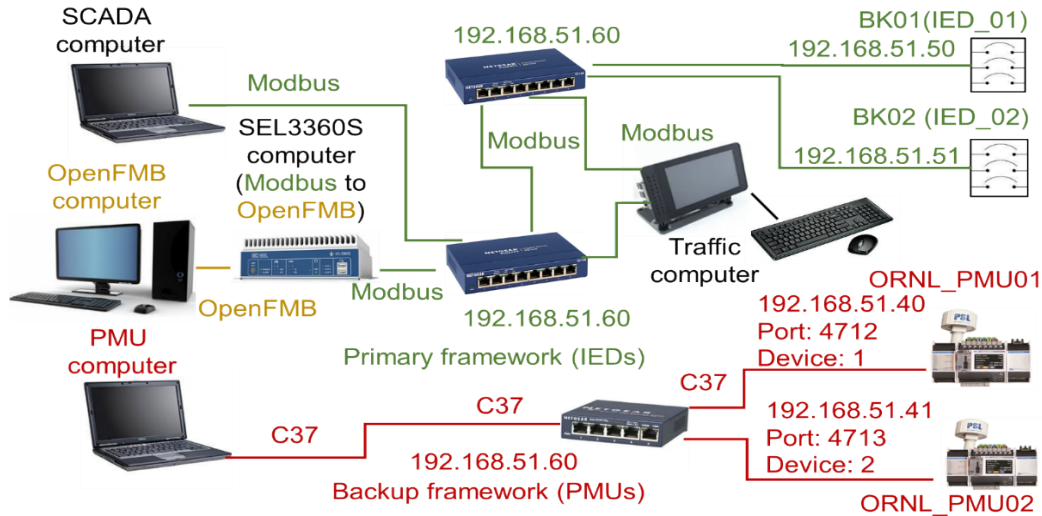


Figure 4: Configuration of the primary and secondary frameworks.

The Modbus protocol was used to integrate the data collected from breakers at the OpenFMB framework, and the C37-118-2011 protocol was used for implementing the DA. The C37-118-2011 protocol was used to estimate the DA because it allows a time stamp and high accuracy data collection [15]. The Synchrophasor system was installed by using the Power Sensors Ltd. instruction manuals [16, 17]. The micro PMUs were wired to the current transformers and the voltages were directly connected to the power line busses. The Global Positioning System (GPS) antennas were connected to the micro PMUs to synchronize measurements, and the consistency of data time stamps was performed by setting the Coordinated Universal Time (UTC) zone for both micro PMUs. The data from the micro PMUs was collected from a Phasor Data Concentrator (PDC) computer. Therefore, the micro PMUs and PDC computer needed to be set in the testbed to collect and estimate the DA at the radial distribution power system. The names, functions and weblinks of the open source software used to set the Synchrophasor system are shown in Table 2.

Table 2: List of synchrophasor software

Names	Functions	Links (Available on June 16, 2019)
microPMU Configurator® [18] v3.6.0.3	- Configure the micro PMUs	https://www.powerstandards.com/download-center/micropmu/?file=5654
PMU Connection Tester® [19] v4.5.11	- Connect one micro PMU - Create the Connection and Configuration files	https://github.com/GridProtectionAlliance/PMUConnectionTester/releases
Open PDC® [20] v2.6	- Concentrate data from several micro PMUs	https://github.com/GridProtectionAlliance/openPDC/releases
FileZilla Client® [21]	- Collect binary data files from micro PMUs	https://filezilla-project.org/
MicroPMU File Converter® [22]	- Convert the micro PMU binary data to CSV files	https://www.powerstandards.com/download-center/micropmu/#4

The software steps for the implementation of the Synchrophasor system are shown in Figure 5. The setting (1-2-3) and data (4-5) collection phases were performed with free download open source software. In the setting phase, the micro PMUs were set with the microPMU® configurator [18] v3.6.0.3 software (1). Then, the data stream for each micro PMU was validated, and the connection and configuration files were created with the PMU Connection Tester® [19] v4.5.11 software (2). The PDC computer was set using the connection and configuration files of the micro PMUs with the Open PDC Manager® [20] v2.6 software (3). In the data collection phase, the binary data from the micro PMUs was collected by the FileZilla Client® [21] software (4), and the binary data files of the micro PMUs was converted into Excel files with the MicroPMU File Converter® [22] software (5). The micro PMU data was converted into excel files to plot the data collected during the tests.

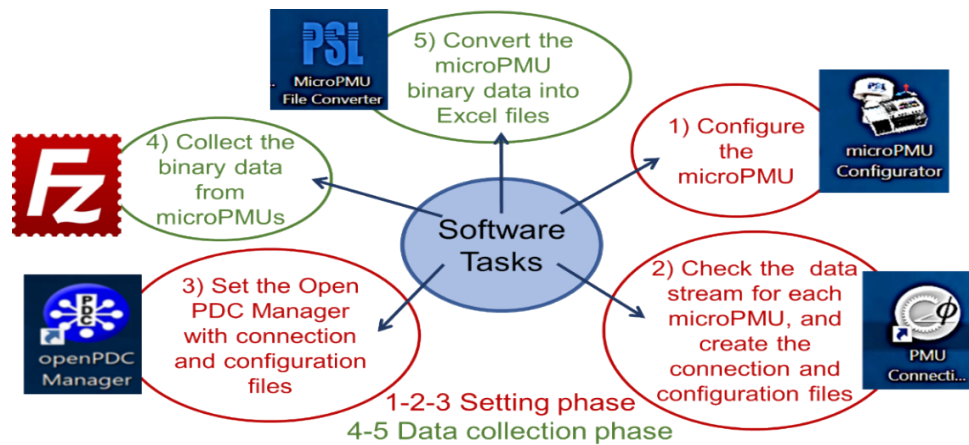


Figure 5: Software steps for the implementation of the Synchrophasor system

3.3 SETTINGS OF MICRO PMUS

The micro PMUs were set with the microPMU Configurator® [18] v3.6.0.3 software. In the micro PMU setting process, the microPMU Configurator® [18] v3.6.0.3 software was opened, and six global default settings were available : PQube general info (1), AC voltage (2), AC currents (3), Network (4), Security (5) and microPMU (6) . At the “PQube general info” menu, the microPMU ID, location name, and notes were set, and the “High Accuracy” option was selected. Figure 6 shows the “PQube general info” settings.

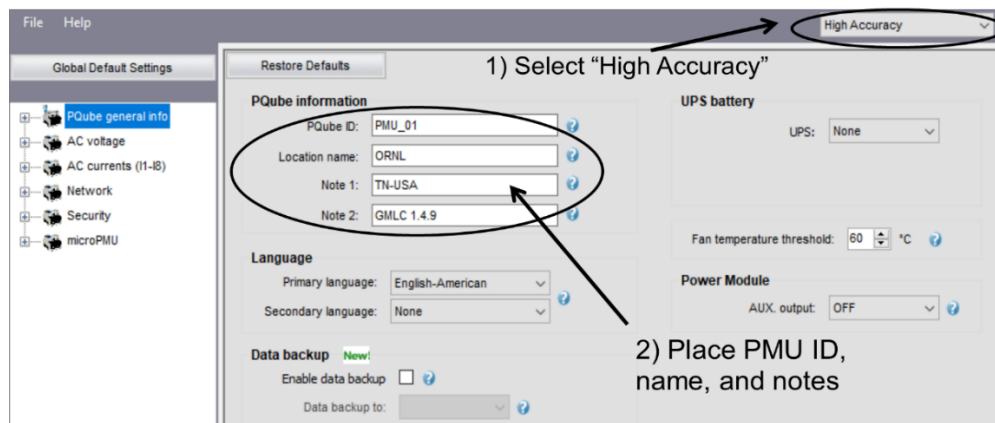


Figure 6: PQube general info setting for “PMU_01” micro PMU

The “AC voltage” menu was set with the nominal frequency (60 Hz), and the potential transformer ratio (1000:1). The “AC currents (I1-I8)” were set with the current transformer ratio (10:1), and the current input range (LOW). The input current range was set at “LOW”, because the current transformers had a full-scale value of 0.333 Vrms. Figure 7 shows the AC voltage and current ratio settings for the micro PMUs.

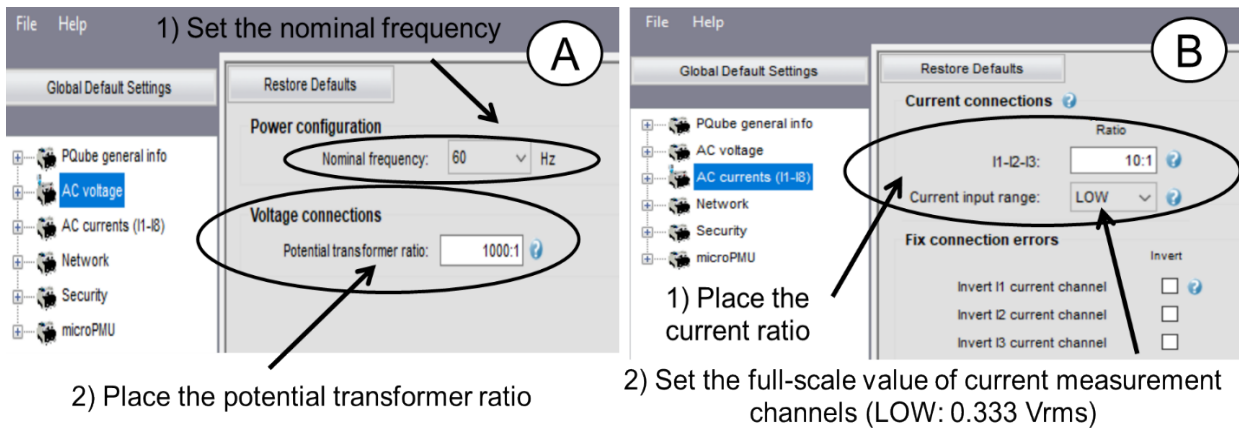


Figure 7: AC voltage (A) and current (B) ratio settings for the micro PMUs

The Network settings for the “PMU_01” micro PMU are shown in Figure 8. The “Network” was set as a fixed IP address, and the IP, mask and gateway addresses for each micro PMU were set. The IP address for the “PMU_01” and “PMU_02” micro PMUs were 192.168.51.40 and 192.168.51.41, respectively. The IP mask and gateway were 255.255.0.0 and 192.168.1.1, respectively. The File Transfer Protocol (FTP) profiles for the micro PMUs were used to record data (ftp_user_1-2-3), upload new setup files (ftp_configuration) and to change the firmware (ftp_updater) for the micro PMUs. The FTP control and data ports were set at 21 and 20, respectively, and the FTP profiles were enabled by setting a password to collect the recorded data from the micro PMUs at end of the simulation tests, by using the FileZilla Client® [21] software.

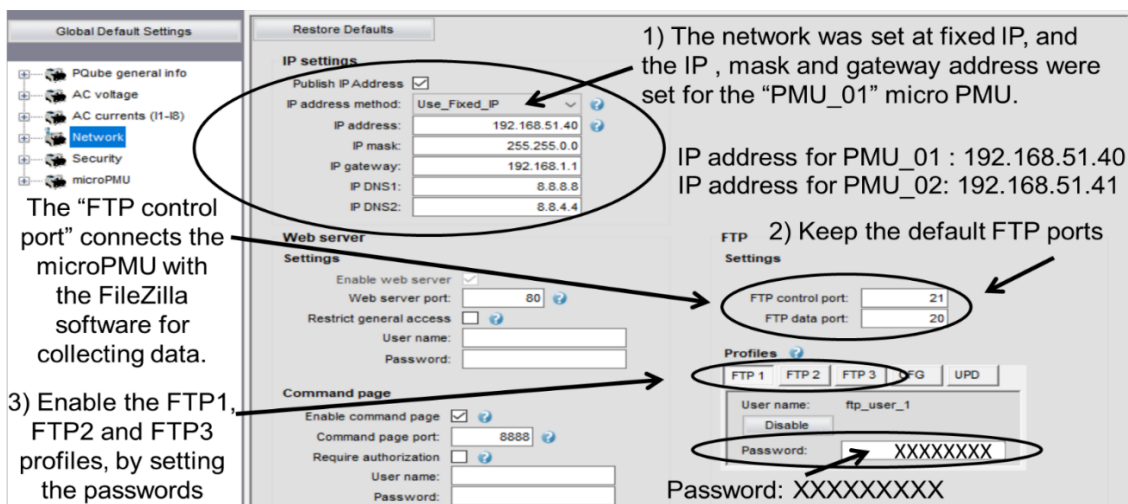


Figure 8: Network settings for the “PMU_01” micro PMU

In the “Security” section, the firewall, web server and the Files Transfer Protocols (FTP) server protection for micro PMUs were available. The “PMU_01” and “PMU_02” micro PMUs were set with the internal firewall protection at the “Security” menu. Figure 9 shows the Security settings for the micro PMUs.

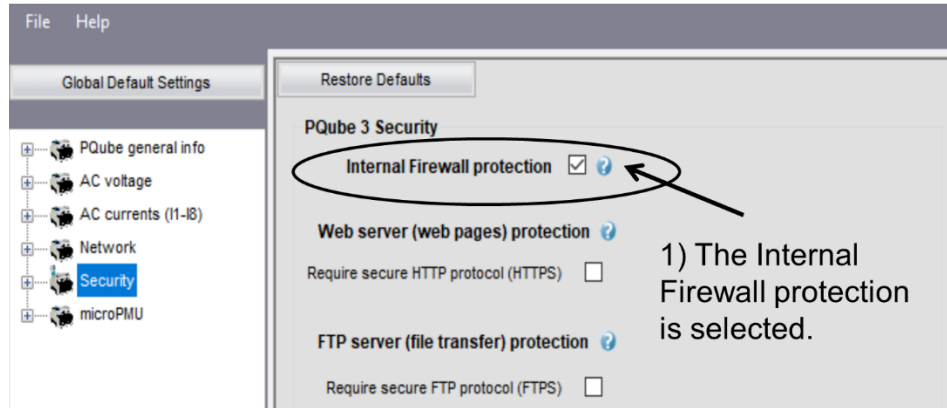


Figure 9: Security settings for the micro PMUs

Figure 10 shows the micro PMU and C37 communication settings for the “PMU_01” micro PMU. In Figure 10- A, the micro PMU settings were set to enable the synchrophasor mode at “HIGH_ACCURRACY”, record 120 samples per second (range 10 to 120 samples per second). The binary file recording period was set at one minute and the frequency and power recording was enabled. In Figure 10-B, the C37 communications settings were set, and the C37 data stream was enabled for recording. The station name, device ID code and port were set for the C37 communication settings. The C37 rate to be transmitted at PDC computer was set at 60 frames per second (range 10 to 120 frames per second). The C37 communication protocol was set at the Transmission Control Protocol (TCP), and the server IP address was set at 192.168.51.60.

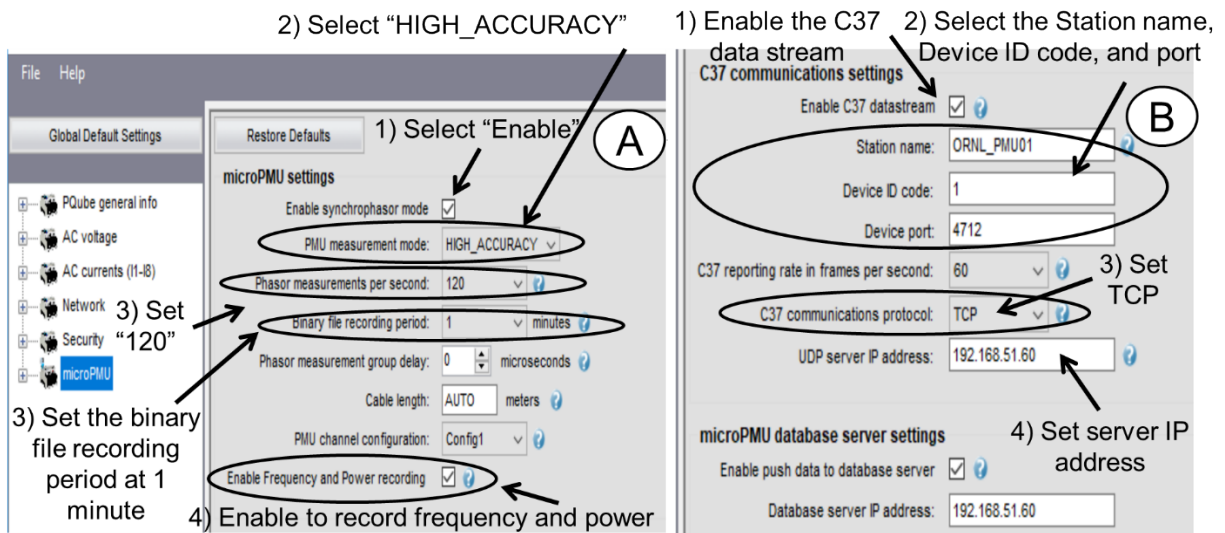


Figure 10: micro PMU (A) and C37 communication (B) settings for the “PMU_01” micro PMU

Once the micro PMU setting was completed, the “File” menu and “Save as” was selected to save the “Setup.ini” file in desktop computer to be downloaded later in the micro PMUs. Figure 11 shows the steps to download and send the “Setup.ini” file to the micro PMU. In the “Setup.ini” file download step, the micro PMU was connected to an ethernet port and computer. The “Setup. Ini” file was downloaded at the micro PMU by using its IP address, and selecting the “Commands” menu and “Download” option. Then, the “Setup,ini” file was browsed from the desktop computer and sent to the micro PMU.

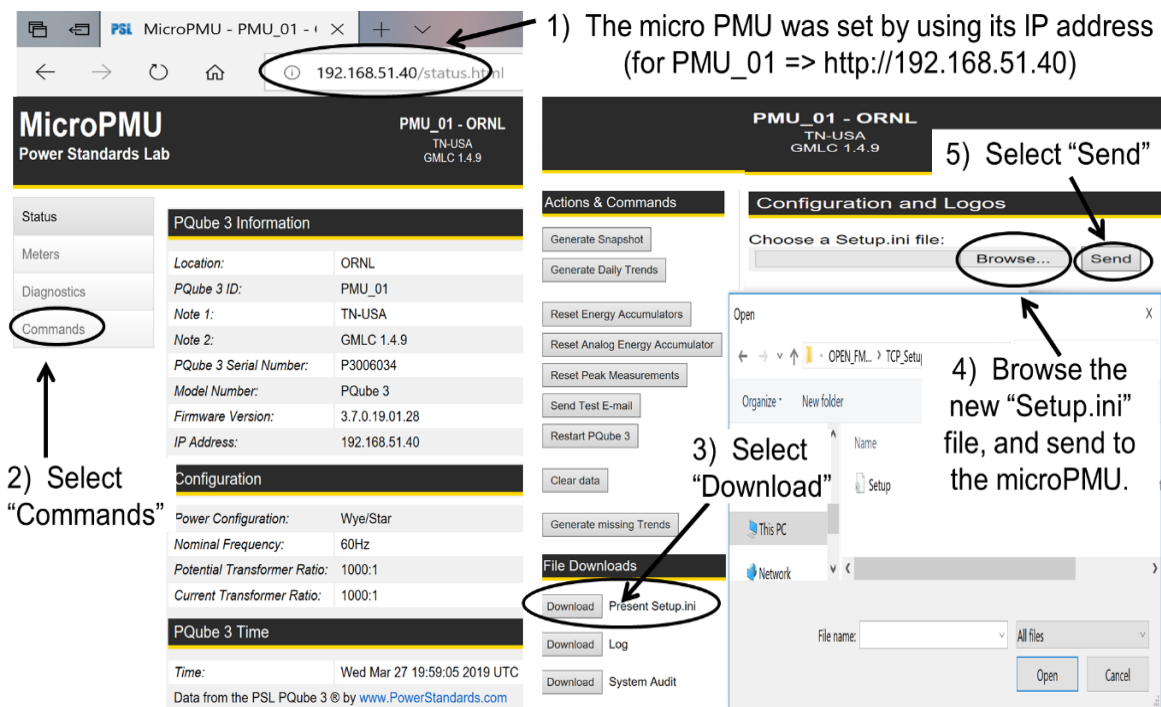


Figure 11: Steps to download and send the “Setup.ini” file to the micro PMU

3.4 SETTING OF PHASOR DATA CONCENTRATOR

The Phasor Data Concentrator (PDC) allowed us to monitor the voltages, currents, and frequency from both micro PMUs at same time during the breaker operation tests. We use a PDC computer with PMU Connection Tester® [19] v4.5.11 and Open PDC® [20] v2.6 software. To set the PDC computer, the connection and configuration files from each micro PMU needed to be collected using the PMU Connection Tester® [19] v4.5.11 software. Then, the communication parameters of the micro PMUs were collected from the micro PMU screens and the “Setup.ini” files. The host IP address of the micro PMUs were collected by selecting the “System” and “Network” icons as shown in Figure 12-A. On the other hand, the type of C37 protocol, and Device Port and ID Code were collected from the “Setup.ini” file downloaded to the micro PMUs as shown in Figure 12-B. Then, the connection of the micro PMU was performed by opening the PMU Connection Tester® [19] v4.5.11 software and using the communication parameters collected previously. Figure 12-C shows the steps to connect with the micro PMU. In the Connection Parameters section, the TCP option was selected, and the host IP address and Port were set. In the Protocol section, the type of C37 protocol and Device ID were set. The Network Interface was selected, and the Ethernet Connection (IP Address: 192.168.51.60) was set. Then, the “Connect” option was selected to communicate with the micro PMU.

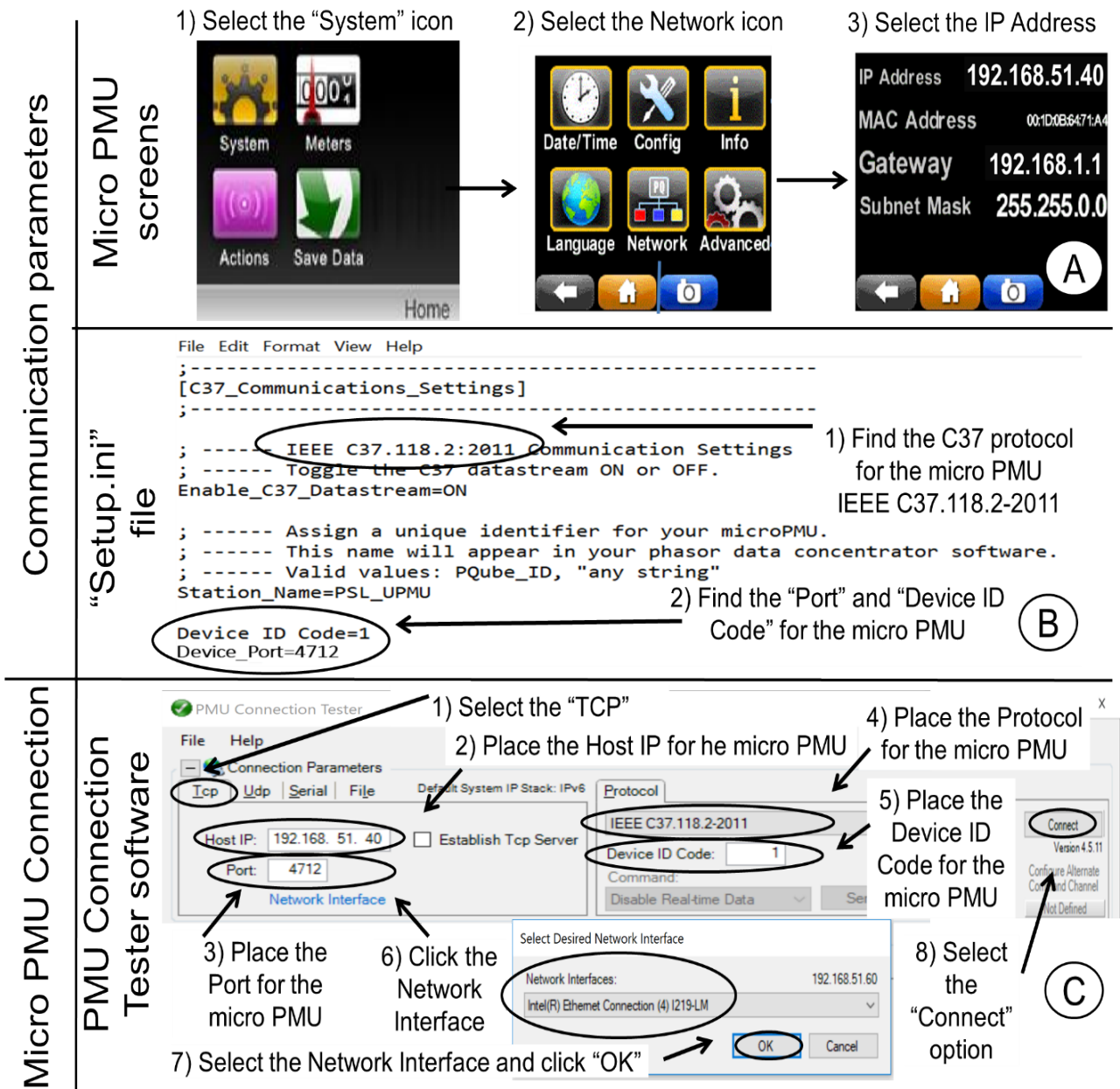


Figure 12: Communication parameters (A-B) and micro PMU connection steps (C)

Once the micro PMU was connected with the PMU Connection Tester® [19] v4.5.11 software, the connection and configuration files from the micro PMU were saved by selecting the "File" menu, and the "Connection" and "Config File" options. The "Connection" and "Configuration" files were saved on the computer's desktop for both micro PMUs for later use to configure the PDC computer. The steps to save the "Connection" and "Configuration" files are shown in Figure 13-A and 13-B, respectively.

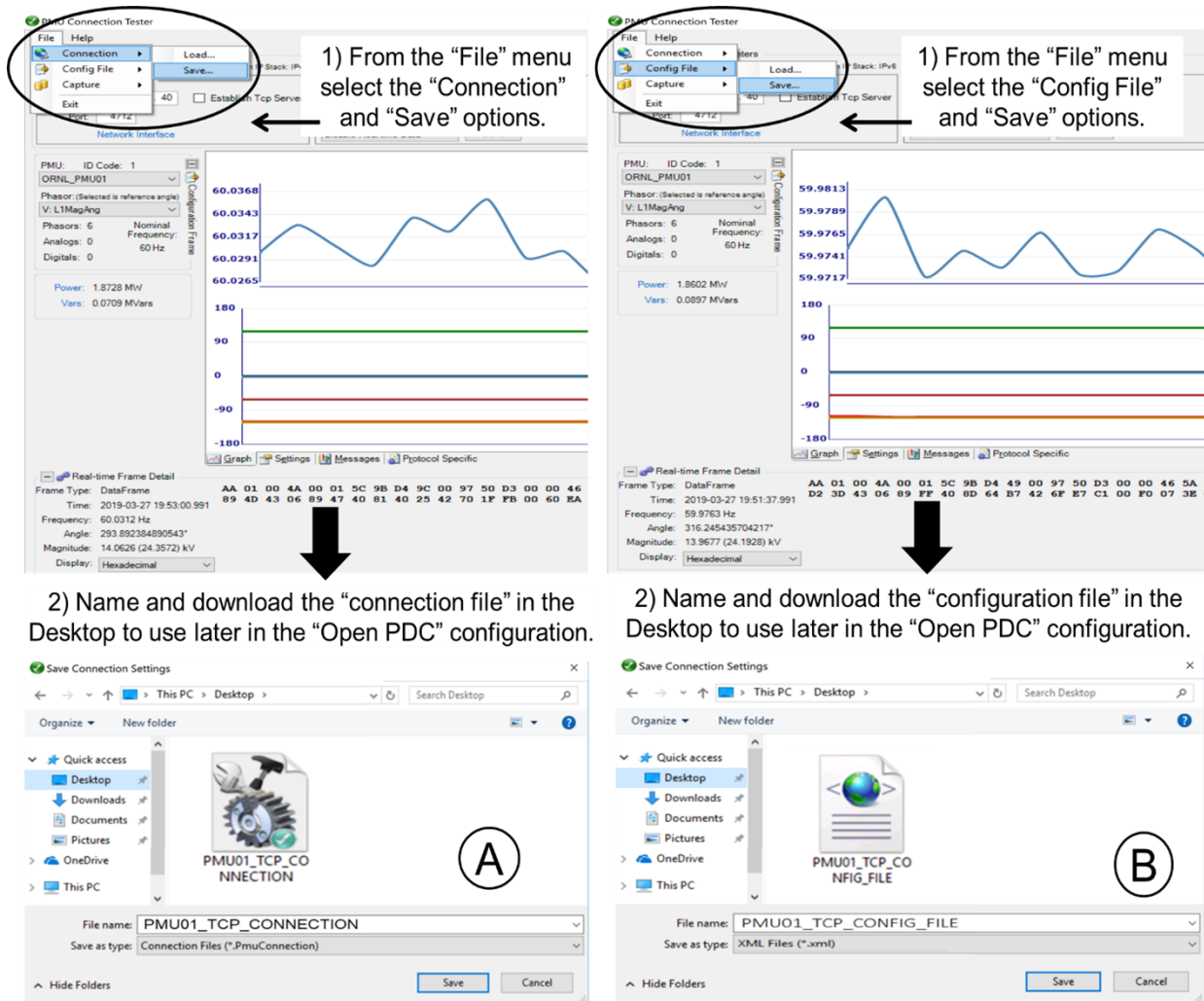


Figure 13: Steps to save the Connection (A) and Configuration (B) files

To configure the PDC computer, the Open PDC® [20] v2.6 software was opened, and the "Inputs" menu and the "Input Device Wizard" option were selected. Figure 14 shows the steps to open the "Input Device Wizard".

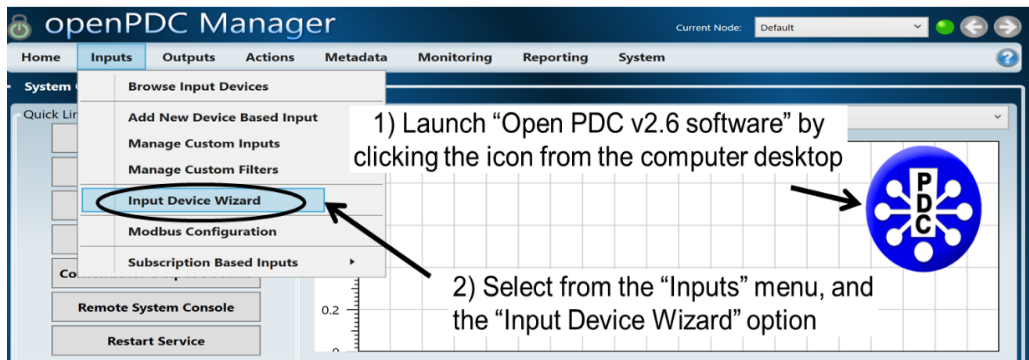


Figure 14: Steps to open the "Input Device Wizard"

Once the “Input Device Wizard” was opened, and the “Launch Walkthrough” was selected, a sequence of windows was performed on the PDC computer screen. The walkthrough guided to fill in the required information by the wizard by selecting the “OK” option (Figure 15-A). It was asked if the device’s connection setting was tested by the PMU Connection Tester® [19] v4.5.11 software, and the “Yes” option was selected (Figure 15-B). After that, it was asked if a Connection file from the PMU connection Tester was available, and the option “Yes” was selected (Figure 15-C). Then, the Browse was selected to find the “Connection” file and save at the “Launch Walkthrough” (Figure 15-D).

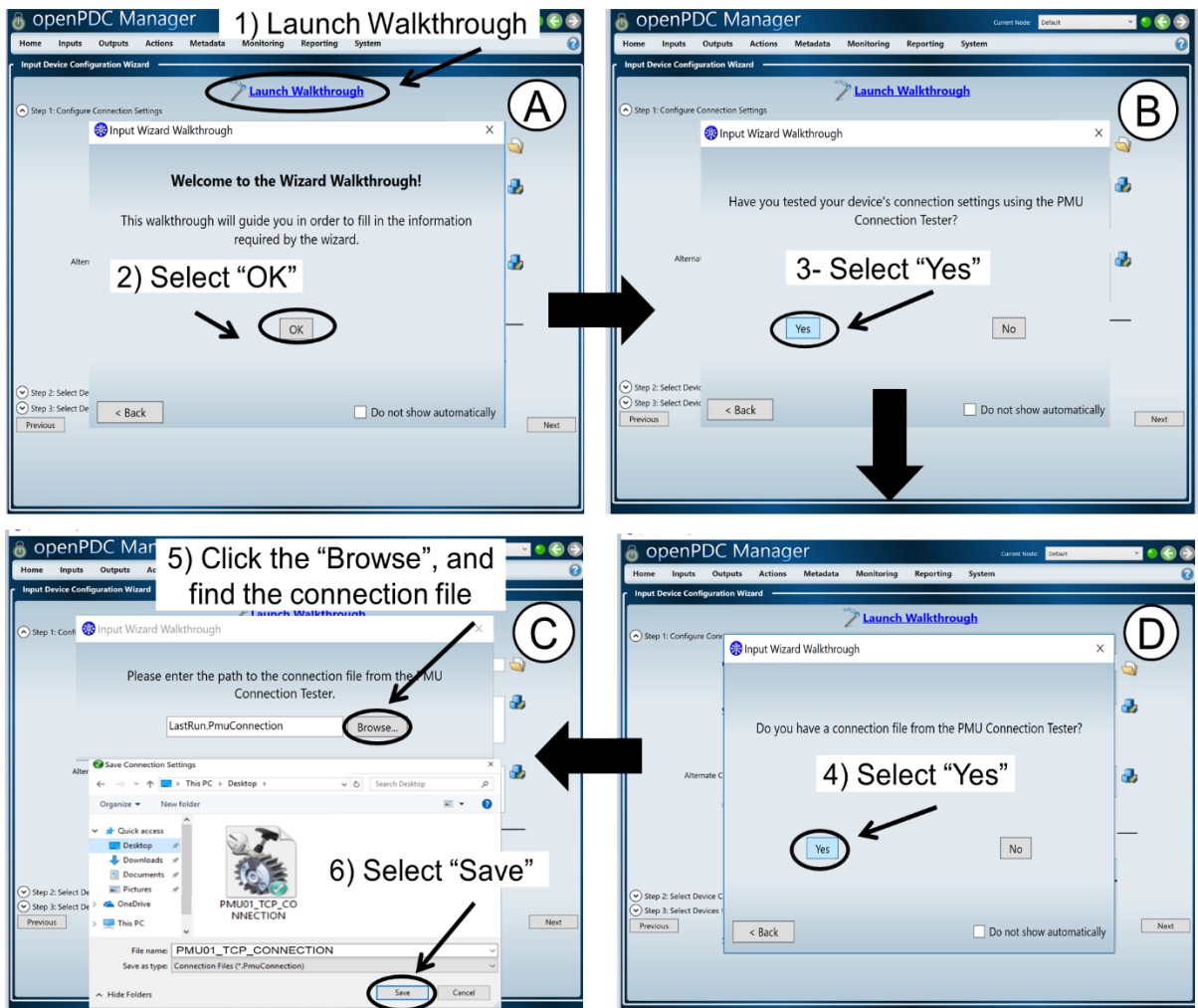


Figure 15: Launch Walkthrough to set the Connection file

The “Launch Walkthrough” was asked if the device was connected to request its configuration, because the Configuration file was saved previously, and “No” was selected to not attempt a device connection (Figure 16-A). The Browse was selected to find the “Configuration” file and save at the “Launch Walkthrough” by selecting “OK” (Figure 16-B). Then, the “Configuration” file was successfully saved (Figure 16-C). The Historian, Company and Interconnection options were left as default, and the “OK” option was selected (Figure 16-D). Then, the “Configuration” information was saved successfully for the “ORNL_PMU01” micro PMU at the Open PDC configuration by selecting the “OK” and “Finish” options (Figure 16-E).

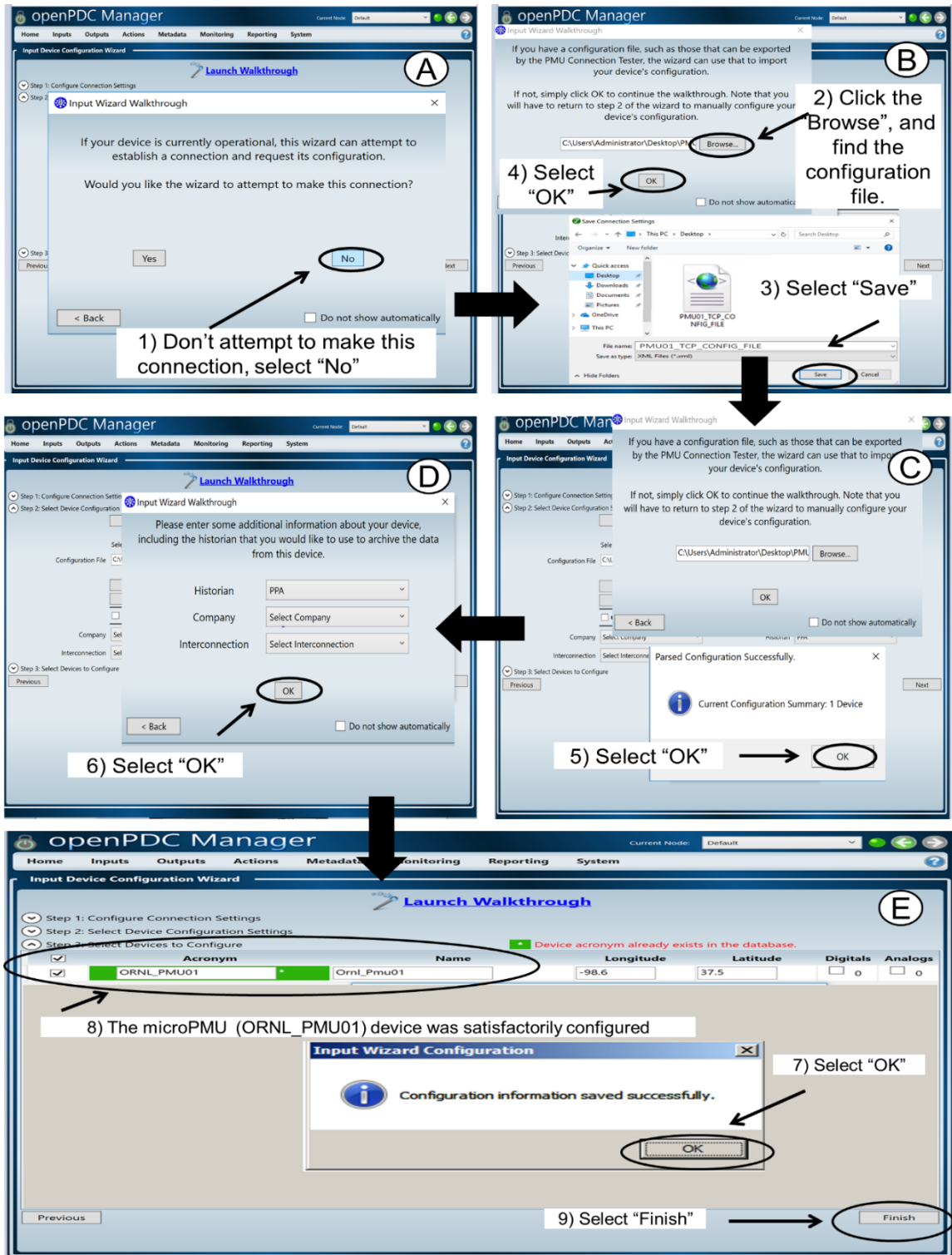


Figure 16: Launch Walkthrough to set the Configuration file

The setting process described for the "ORNL_PMU01" micro PMU by using the Open PDC® [20] v2.6 software, was performed by selecting the "Input Device Wizard" and "Launch Walkthrough" options. This process was also repeated for the "ORNL_PMU02" micro PMU in order to configure all devices at the PDC computer.

3.5 MONITORING THE MICRO PMUS

The micro PMUs were monitored from the Phasor Data Concentrator (PDC) computer after the micro PMUs were configured successfully with the Connection and Configuration files. Then, voltages, currents, and frequency were measured by enabling the data stream from the micro PMUs. The Open PDC® [20] v2.6 software was opened, and the “Inputs” menu was selected as shown in Figure 17-A. The “Enabled” box was selected to permit the stream data from the “ORNL_PMU01” micro PMU, and the “ORNL_PMU01” device was selected at the “Acronym” column, to open the “Manager Device Communication” window.

The “Manger Device Communication” window was opened as shown in Figure 17-B. The C37.118.2-2011 protocol was selected based on the “Setup.ini” file used to set the “ORNL_PMU01” micro PMU, and the download “Connection String” was checked to verify the TCP, server (19), port (4712) and interface (192.168.51.60) for the “ORNL_PMU01” micro PMU. Then, the “Skip Disable Real-time Data” box was selected, to enable the real-time date from the micro PMU. The process detailed in this section was also performed for the “ORNL_PMU02” micro PMU in order to enable all devices. Figure 17 shows the steps to enable the data stream for the “ORNL_PMU01” micro PMU.

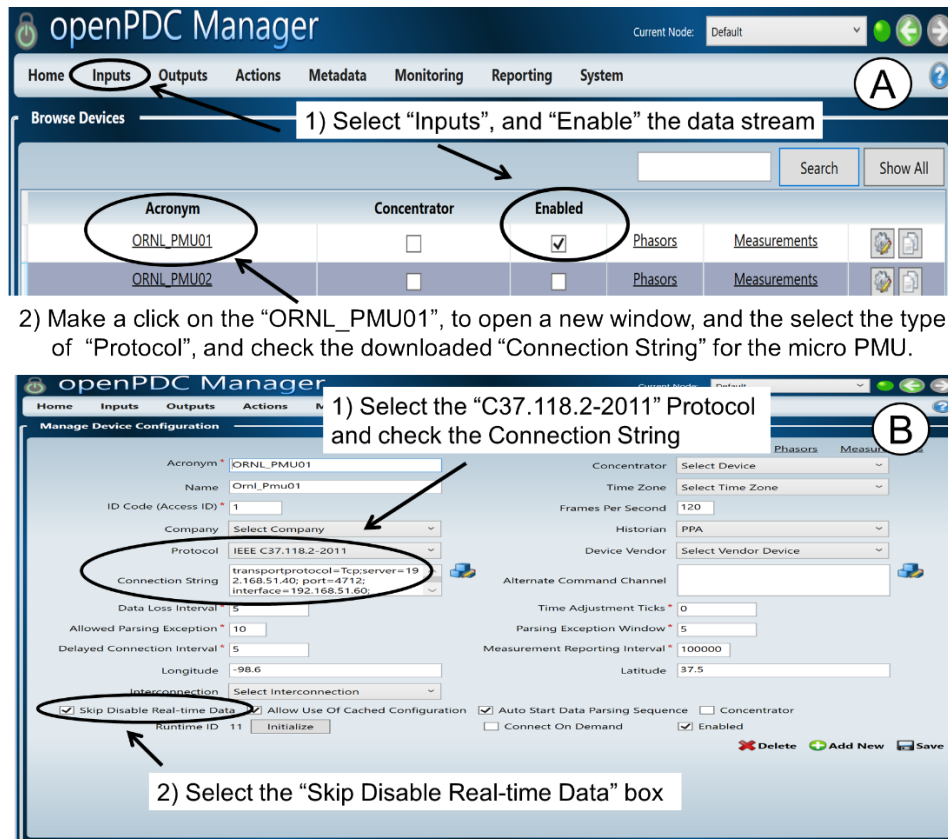


Figure 17: Steps to enable the data stream of micro PMUs

After the data stream from the micro PMUs was enabled at the Open PDC system, the frequency, phase and magnitude of voltages and currents were selected to be plotted in real time. The “Home” menu and the “Graph Measurements” link were selected to see the available data stream from the micro PMUs (Figure 18-A and B). The frequency system (ORNL_PMU01-FQ) and Line 1 Voltage Phase Angle (ORNL_PMU01-PA1) for the “ORNL_PMU01” micro PMU were selected to be plotted in a graph in real time (Figure 18-C). The “Display Settings” option was selected to set the horizontal (X) and vertical (Y)

axis of the graph. The frequency range was set between 59.99 and 60.01 Hz, and the “Display Frequency” and “Phase Angle” at Y-Axis were selected (Figure 18-C).

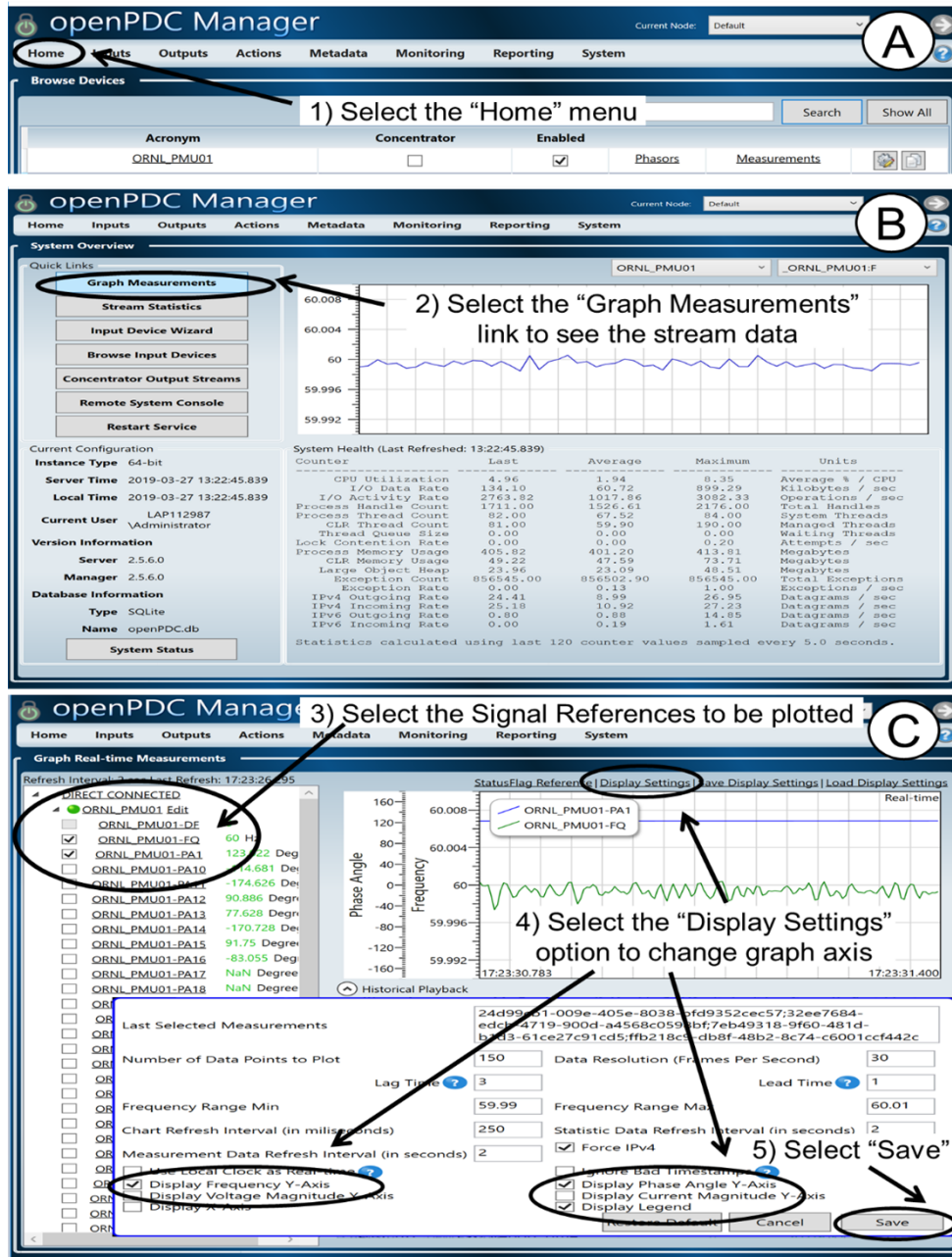


Figure 18: Steps to plot the stream data from micro PMUs

The “Descriptions” of the “Signal References” that were plotted (Figure 18-C) could be found by selecting the “Inputs” menu, and the “Measurements” option for the “ORNL_PMU01” micro PMU (Figure 19-A). The ID “Description” was selected to find the “Signal Reference” above (Figure 19-B). In Figure 19-B, the “Ornl_Pmu01_L1MagAng + Voltage Phase Angle” Description was the “ORNL_PMU01-PA1” Signal Reference that corresponded to the Line 1 Voltage Phase Angle. In addition, all the Descriptions of Signal References from the “ORNL_PMU01” and “ORNL_PMU02” micro PMUs could be found based on the steps are shown in Figure 19.

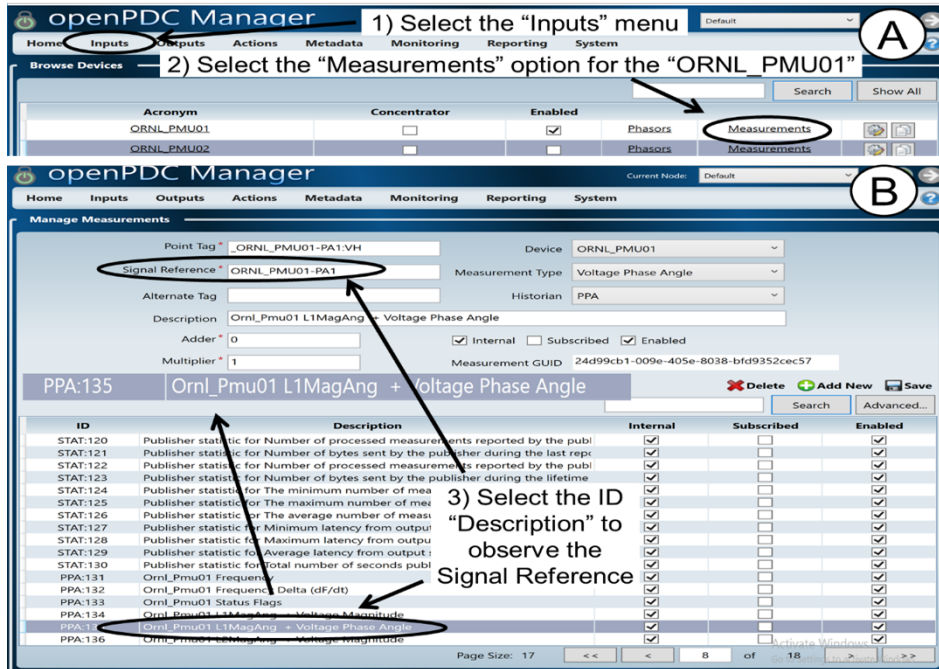


Figure 19: Steps to find the Description of Signal References for the micro PMUs

3.6 COLLECTING THE DATA FROM THE MICRO PMUS

The collection of data from the “ORNL_PMU01” and “ORNL_PMU02” micro PMUs was performed after running the breaker operation tests. The FileZilla Client® [21] software was used to collect the data recorded by the micro PMUs, and the microPMU File Converter® [22] software was used to convert the micro PMU recorded binary data to CSV (Excel) files. To collect the binary data from the micro PMUs, the FileZilla Client® [21] software was opened from the PDC computer after running all tests. Then, the Host, Username, Password and Port for the micro PMU were filled in, and the “Quickconnect” and “OK” options were selected as shown in Figure 20.

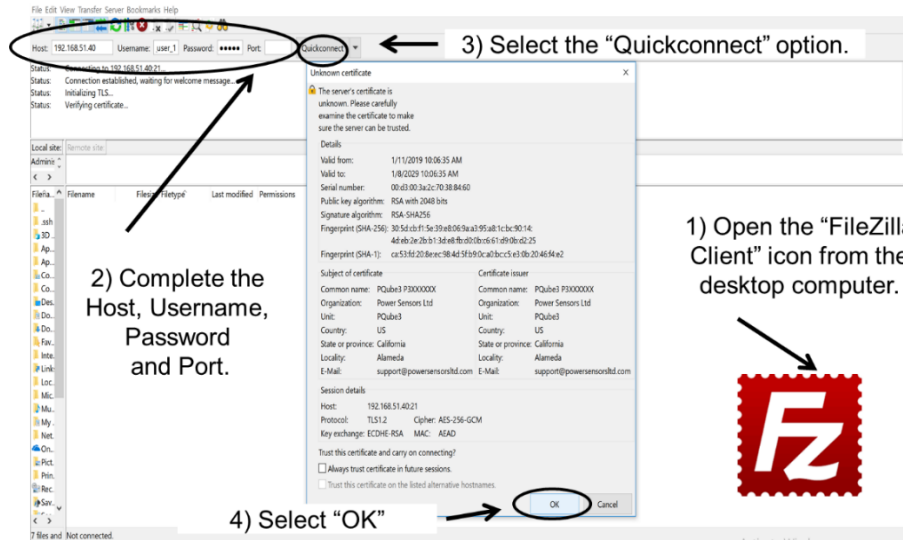


Figure 20: Steps to communicate with micro PMUs by the FileZilla Client® [21] software

Table 3 shows the communication parameters to collect the binary data with the FileZilla® Client [21] software from the PDC computer, after running the real-time tests for the ORNL_PMU01 and ORNL_PMU02 micro PMUs.

Table 3: Communication parameters to collect binary data from the micro PMUs

Micro PMUs	Host	Port	Usernames
ORNL_PMU01	192.168.51.40	21	ftp_user_1, ftp_user_2, ftp_user_3
ORNL_PMU02	192.168.51.41		

In the micro PMUs, the collected data was synchronized with the Universal Coordinated Time (UTC), and the phasor data was saved as “binary.dat” files stored in folders that were arranged by Year, Month, Day, Hour and Minute. During the breaker operation tests, the micro PMU screens were saved to record the time when tests were run, and to find the binary data files at the micro PMUs. The “upmu_data” folder was opened to collect the “year_month_day_hour” file (Figure 21-A). Then, the “year_month_day_hour” file was saved in the desktop computer (Figure 21-B). The steps to download the binary data files from the micro PMUs are shown in Figure 21.

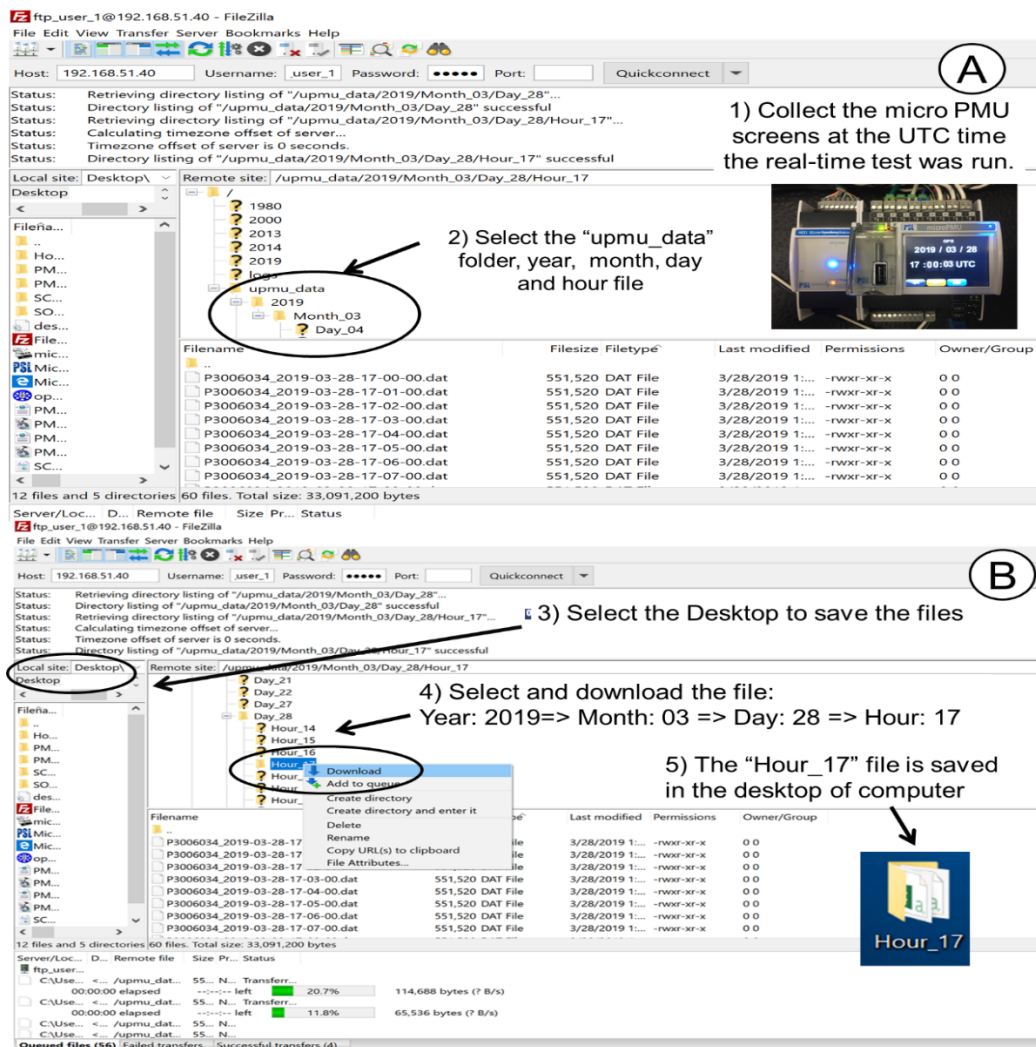


Figure 21: Steps to download the binary data files from the micro PMUs

Figure 22 shows the steps to convert the “binary.dat” into an “Excel” files for micro PMUs. The stored “binary.dat” file was converted into an Excel file with the MicroPMU File Converter® [22] software. The MicroPMU File Converter® [22] software was opened, then the microPMU location was set, and the stored and destination of folders were selected, to convert the “binary.dat” files into an Excel files (Figure 22-A). Once the files were converted successfully, the “Minute” Excel file for the breaker operation test was opened to analyze the voltages, currents, power, displacement power factor and frequency from the micro PMU (Figure 22-B).

1) The “MicroPMU File Converter” software was opened.

2) Enter the microPMU location

3) Choose the folder on your computer where the binary files are stored

4) Choose a destination folder for your CSVs

5) Click the “Convert .dat files to .csv (Excel) files” button

6) Click “OK”

7) The “Hour_17” test file was opened

8) Collect the “Minute” when the real-time test was run.

9) Open the Excel file to analyze collected data

sample	indate	stamp	time	status	L1-E	L2-E	L3-E	L1-current	L2-current	L3-current	center	freq	discipline	pl	state				
5	8.333333	3/28/2019	00:00.0	38	330.7245	0.116806	336.3896	0.348781	335.4413	0.39409	4.98E-11	303.6727	0.002132	184.3256	0.001548	85.0298	17	4	1
6	8.333333	3/28/2019	00:00.0	38	191.3692	7.429176	189.655	7.544107	192.8905	6.954975	4.44E-11	123.8932	0.006797	350.2147	0.009603	163.3468	17	4	1
7	8.333333	3/28/2019	00:00.0	38	133.1091	359.9608	334.2636	359.9535	339.4138	0.017256	3.59E-11	303.6994	0.005171	177.9603	0.007147	82.16357	17	4	1
8	8.333333	3/28/2019	00:00.0	38	190.6196	7.717073	189.2184	7.809742	192.7417	7.320831	2.71E-11	123.7963	0.008186	36.3564	0.004278	12.40159	17	4	1
9	8.333333	3/28/2019	00:00.0	38	327.0078	359.2469	332.1924	359.6005	334.8546	358.6364	1.93E-11	303.5642	0.000978	237.7181	0.011794	86.01811	17	4	1
10	8.333333	3/28/2019	00:00.0	38	185.4186	7.982804	191.7842	7.886408	197.3959	6.888556	1.44E-11	123.1194	0.004855	213.9431	0.012879	90.27824	17	4	1
11	8.333333	3/28/2019	00:00.1	38	331.9522	359.7981	330.4749	359.9504	339.2503	359.5488	1.05E-11	303.3034	0.002419	172.085	0.004545	330.1743	17	4	1
12	8.333333	3/28/2019	00:00.1	38	185.6282	7.941436	190.9607	6.77237	191.5741	7.558204	5.61E-12	124.2198	0.005576	107.7002	0.009731	83.41724	17	4	1
13	8.333333	3/28/2019	00:00.1	38	334.493	359.5699	340.2242	359.4865	338.7519	358.7307	1.49E-12	300.7788	0.010623	180.9589	0.009235	95.83873	17	4	1
14	8.333333	3/28/2019	00:00.1	38	187.5248	7.806319	188.3796	8.215368	197.5307	6.36425	2.21E-12	216.6688	0.001975	190.4473	0.00882	83.01608	17	4	1
15	8.333333	3/28/2019	00:00.1	38	332.7437	359.0269	331.5909	358.7526	335.3166	358.9691	1.21E-12	219.9353	0.004581	107.204	0.004004	230.2661	17	4	1
16	8.333333	3/28/2019	00:00.1	38	185.0782	7.631987	196.15	6.715219	198.3874	6.397327	1.52E-12	116.3606	0.009338	131.227	0.009004	227.851	17	4	1
17	8.333333	3/28/2019	00:00.1	38	331.3062	358.7533	334.8025	358.8274	335.687	358.192	9.45E-14	232.1877	0.001393	114.4421	0.007839	56.22468	17	4	1
18	8.333333	3/28/2019	00:00.1	38	185.4866	6.415963	189.4076	5.98659	193.8906	4.862401	2.25E-12	2.497985	0.007365	191.2929	0.005845	54.51935	17	4	1
19	8.333333	3/28/2019	00:00.1	38	330.2115	359.6428	334.3475	359.2835	332.6986	359.0205	1.26E-12	261.7265	0.009347	268.9431	0.012351	196.3049	17	4	1
20	8.333333	3/28/2019	00:00.1	38	191.069	7.416785	194.8258	5.460189	195.9438	6.534494	2.88E-12	183.9442	0.005326	307.0516	0.008531	140.4366	17	4	1

Figure 22: Steps to convert “binary.dat” into an “Excel” file for micro PMUs

4. DATASETS AND EXPERIMENTS

We conducted experiments to explore what features can be collected and feasibly shared using the OpenFMB data model and what features would be useful to add to an analytics OpenFMB data model. Several types of data were generated from these experiments. Three main datasets were created. The main sensors on the two switches and the load bank were recorded using Modbus and transmitted over OpenFMB and then collected into CSVs, mPMUs were also used and recorded data onto sd cards and over OpenPDC. Network traffic captures in the form of pcaps were also created by using the span port on a switch configured to mirror all incoming and outgoing traffic from all ports. Table 4 shows how the experiments were carried out.

Table 4: Description of experiment datasets

Data
OpenFMB sensors/ mPMU/ Network traffic
Normal Operation
Open and close breaker 1 then open and close breaker 2
Ping flood experiments
Ping flood breaker 1
Ping flood breaker 2
Ping flood loadbank
Ping flood pmu 1
Ping flood pmu 2
SYN flood experiments
SYN flood port 80 breaker 1
SYN flood port 80 breaker 2
SYN flood port 80 load bank
SYN flood port 80 pmu 1
SYN flood port 80 pmu 2
UDP flood experiments
Udp flood port 80 breaker 1
Udp flood port 80 breaker 2
Udp flood port 80 load bank
Udp flood port 80 pmu 1
Udp flood port 80 pmu 2
Cable disconnect
Cable disconnect breaker 1
Cable disconnect breaker 2
Cable disconnect loadbank
Cable disconnect pmu 1
Cable disconnect pmu 2

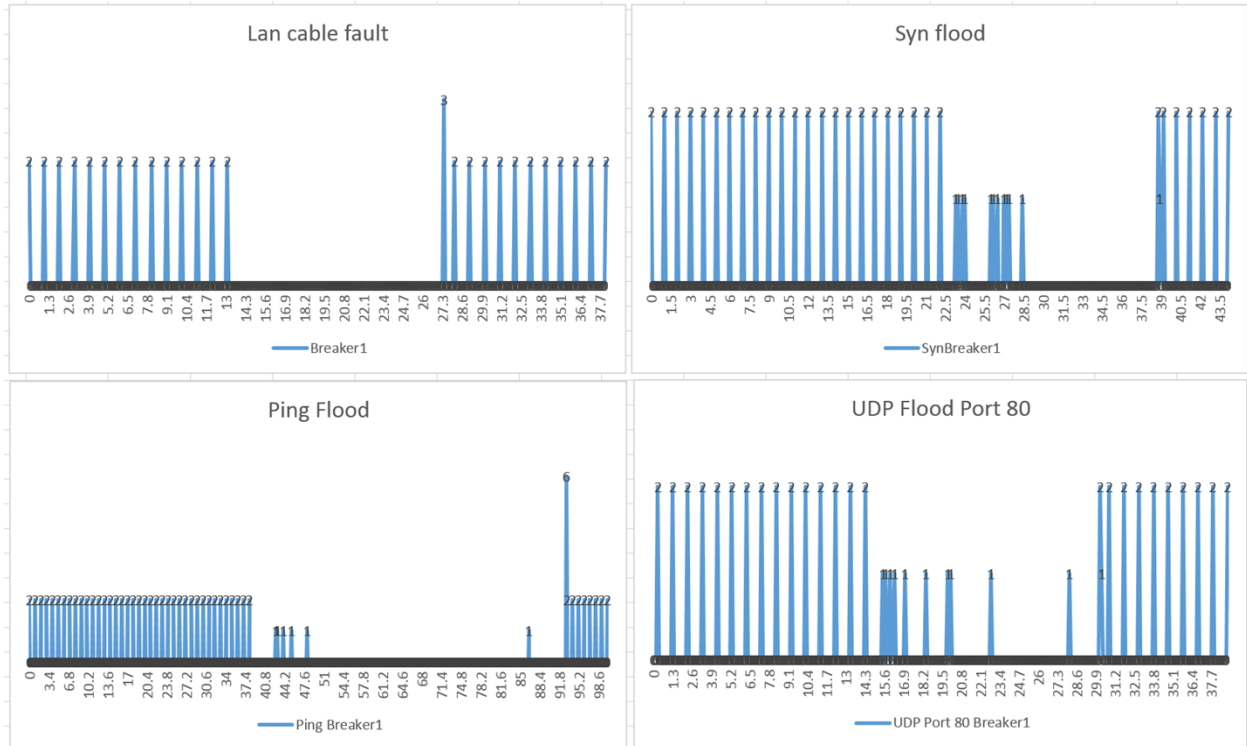


Figure 23: Impact on Modbus traffic based on data IO in packets per 100ms for each experiment

Figure 23 shows four graphs of the behavior of the Modbus connection for Breaker 1 under various types of network experiments. LAN cable fault is done simply disconnecting the LAN cable, SYN flood is creating a SYN flood directed at breaker 1. SYN floods attempt to establish a TCP SYN handshake but never finish and therefore leave the connection open and attempt to open tens of thousands this way. Ping flood is a barrage of ICMP packets and UDP flood is like a SYN flood but using UDP packets instead of TCP. In the absence of an initial handshake, to establish a valid connection, a high volume of “best effort” traffic can be sent over UDP channels to any host, with no built-in protection to limit the rate of the UDP DoS flood. This means that not only are UDP flood attacks highly effective, but also that they could be executed with a help of relatively few resources [32]. The main difference noticed during the experiments was the instant cutoff for the cable disconnect versus the slow decline of traffic caused by DoS attacks.

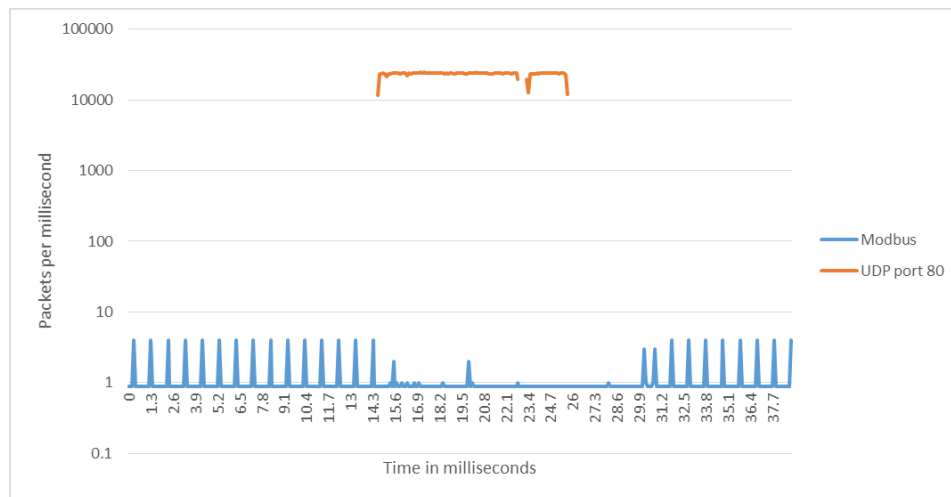


Figure 24: UDP packet flood effect on breaker 1 Modbus network responsiveness

In Figure 24 we see the UDP flood effect on the Modbus traffic. As the attack starts the Modbus responsiveness slowly starts to decline. Unless network traffic features are incorporated into the OpenFMB analytics model the type of analytics needed to share warnings to edge devices would need to come from a centralized intrusion detection system [33].

4.1 AVAILABLE MICRO PMU DATA FOR ANALYTICS

The available DA estimated by micro PMUS are the voltages, currents, power, displacement power factor and frequency [16]. In the “PMU_01” and “PMU_02” micro PMUs, the collected data from the micro PMUs had a sample interval of 8.33 milliseconds that represents the time between which data are recorded. The micro PMUs sense the voltage and current RMS fundamental magnitude and angle for L1, L2 and L3 phases using a common time source for synchronization. Table 5 shows the fundamental voltages, currents, frequency, and total true, reactive and apparent power, and displacement power factor that are estimated by the micro PMUs.

Table 5: Data analytics estimated by the micro PMUs

Voltages, Currents and Frequency

<i>Phases</i>	<i>Line-to-Ground Voltages [volts]</i>	<i>Line Currents [amps]</i>	<i>Frequency [Hz]</i>
L1	L1-E voltage RMS fundamental magnitude (V_{L1})	L1-E current RMS fundamental magnitude (I_{L1})	frequency one second (F_{L1})
	L1-E voltage fundamental angle (Θ_{VL1})	L1-E current fundamental angle (Θ_{IL1})	frequency C37 (F_{L1-C37})
L2	L2-E voltage RMS fundamental magnitude (V_{L2})	L2-E current RMS fundamental magnitude (I_{L2})	-
	L2-E voltage fundamental angle (Θ_{VL2})	L2-E current fundamental angle (Θ_{IL2})	-
L3	L3-E voltage RMS fundamental magnitude (V_{L3})	L3-E current RMS fundamental magnitude (I_{L3})	-
	L3-E voltage fundamental angle (Θ_{VL3})	L3-E current fundamental angle (Θ_{IL3})	-

True, Reactive, Apparent Power and Displacement Power Factor

fundamental total true power (W) [wattss]	Fundamental total reactive power (VAR) [vars]	fundamental total apparent power (VA) [volts-amps]	fundamental total displacement power factor (dPF)
---	---	--	---

Eq. (1)

Eq. (2)

Eq. (3)

Eq. (4)

The micro PMU also calculated the frequency one second and frequency C37 at L1 phase (A phase). The fundamental total true, reactive and apparent power were calculated by measuring the voltages and currents of L1 (A phase), L2 (B phase) and L3 phase (C phase) from the micro PMUs. The fundamental total true power (W) was estimated by (1).

$$W = \sum_{n=1}^3 V_{Ln} \times I_{Ln} \times \cos(\theta_{VLn} - \theta_{ILn}) \quad (1)$$

where V_{Ln} is the voltage RMS fundamental magnitude at n phase in volts, I_{Ln} is the current RMS fundamental magnitude at n phase in amps, θ_{VLn} is the voltage fundamental angle at n phase in degrees, and θ_{ILn} is the current fundamental angle at n phase in degrees.

The fundamental total reactive power (VAR) was estimated by (2).

$$VAR = \sum_{n=1}^3 V_{Ln} \times I_{Ln} \times \sin(\theta_{VLn} - \theta_{ILn}) \quad (2)$$

The fundamental total apparent power (VA) was estimated by (3).

$$VA = \sum_{n=1}^3 V_{Ln} \times I_{Ln} \quad (3)$$

The fundamental total displacement power factor (DPF) was estimated by the micro PMUs. The dPF is the power factor due to the phase shift between voltage and current at the fundamental line frequency. For sinusoidal (non-distorted) currents, the displacement power factor is the same as the apparent power factor. Then, the fundamental total DFP was estimated by (4).

$$dPF = W / VA \quad (4)$$

4.2 OPENFMB DATA

The available OpenFMB data collected is in the form of CSV files read with a backend python application that sits on the back of an OpenFMB profile for reading sensor values from relays. We were able to implement two different OpenFMB profiles to read from the two relays and the sbRIO connected to the load bank using Modbus. The format has Voltage, Current and Power measurements for all 3 phases and for both load side and source side. The log also records the OpenFMB Modbus read timestamp, local log read timestamp and OpenFMB pub/sub topic subject being either Resource Reading profile or Switch Reading.

4.3 PCAP DATA

The network traffic recorded captures all possible packets for all devices including the micro PMUs and engineering workstations controlling the relays and programmable load bank. We evaluate the network traffic for its’ potential use as a feature for analytics and determining whether OpenFMB’s data analytic profile should also contain features for sharing network traffic characteristics, for use in machine learning. Network traffic is widely used for intrusion detection systems. Given that many of the same attacks performed on traditional IT systems carry over into the industrial control (ICS) space We include it as a custom subcomponent in an existing OpenFMB data model. Packet interarrival time provides among other network traffic features a useful feature for detection of Denial-of-service attacks which are also a danger to ICS systems.

5. RESULTS

5.1 TEST AND COLLECTED DATA FOR ANALYTICS

The available micro PMU data was based on the fundamental currents (L1, L2 and L3), voltages (L1-E, L2-E and L3-E), frequency (C37 L1-E and one second L1-E), and total true, reactive and apparent power, and displacement power factor. In the power system simulation, the breaker operation tests were performed by closing, opening and closing the “BK01” and “BK02” breakers at the beginning of the parallel power line, and data from the “ORNL_PMU01” and “ORNL_PMU02” micro PMUs were collected with a sample interval of 8.333333 milliseconds (two samples per cycle for a 60 Hz signal – sample rating of 120 samples per seconds). Figure 25 shows the circuit and the sequence for breaker operation tests.

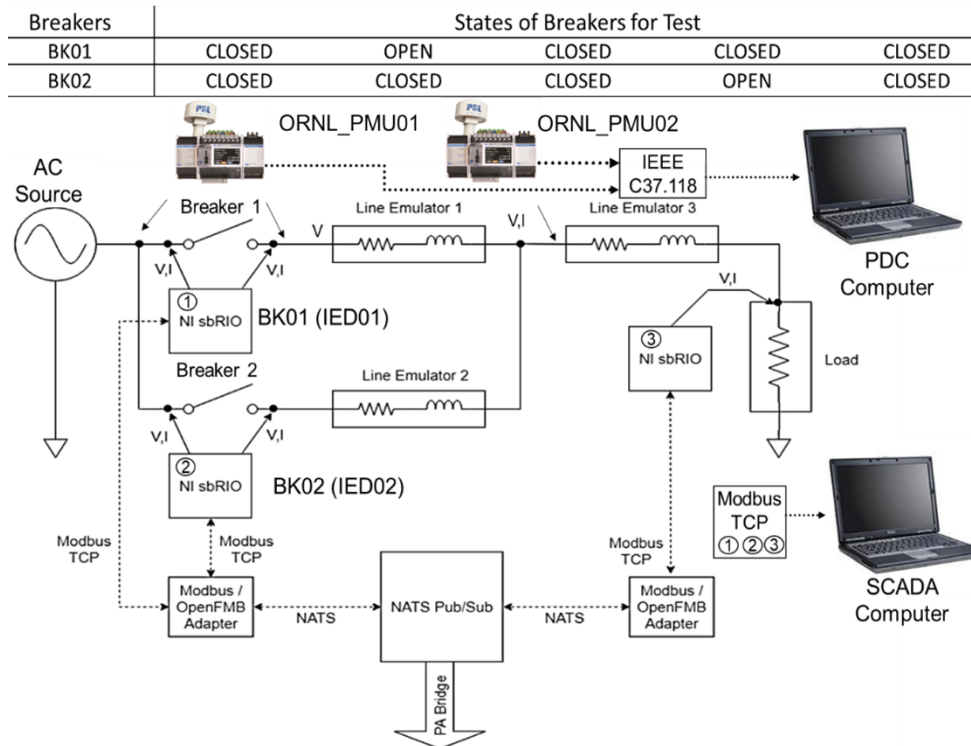


Figure 25: Circuit and sequence for breaker operation tests

The micro PMUs were set at different Coordinated Universal Time (UTC) zone because they were located at the beginning and end of the parallel power line. Figure 26 shows the initial and final time when the breaker operation tests were performed in order to collect the data from the “ORNL_PMU01” and “ORNL_PMU02” micro PMUs. The data from the “ORNL_PMU01” and “ORNL_PMU02” micro PMUs were collected at 2019/05/28 (year/ month/day) at 21: 00 hours and 02-03 and 00-01 minutes, respectively.

Devices	ORNL_PMU01	ORNL_PMU02
Locations	Beginning of parallel power lines	End of parallel power lines
Initial test time		
Final test time		

Figure 26: Initial and final test times from the “ORNL_PMU01” and “ORNL_PMU02” micro PMUs

5.1.1 Data from the “ORNL_PMU01” micro PMU

The data from the “ORNL_PMU01” micro PMU was collected at the breaker operation tests. The “ORNL_PMU01” was installed at the beginning of the parallel power lines, and it measured the currents for the “BK01” breaker, and voltages of bus at the energy three-phase source. The fundamental L1 current and L1-E voltage magnitudes were plotted in Figure 27-A and B, respectively. The fundamental L1 current magnitude was four amperes when “BK01” and “BK02” breakers were closed, because both parallel power lines feed the controllable resistive load bank. The fundamental L1 current magnitude was zero amperes when “BK01” and “BK02” breakers were opened and closed respectively, because no current was flowing through the “BK01” breaker.

The fundamental L1 current magnitude was eight amperes when “BK01” and “BK02” breakers were closed and open respectively, because only the power line connected to “BK01” was feeding the controllable resistive load bank. The fundamental L1 current and L1-E voltage angles were plotted in Figure 27-C and D, respectively. While the fundamental L1-E voltage angle was almost similar when the BK01 and BK02 were opened and/or closed, because the fundamental L1-E voltage angle was measured at the power source. The fundamental L1 current angle showed an oscillation between 360 and 0 degrees when the “BK01” was opened. The fundamental L1 current angle measured by the “ORNL_PMU01” micro PMU had a noise that was produced by the open state of “BK01” breaker. This situation should be

considered when a decision based on DA is implemented using the L1 current angle from the micro PMUs, to avoid non-desired DA estimations between electrical utilities and customers.

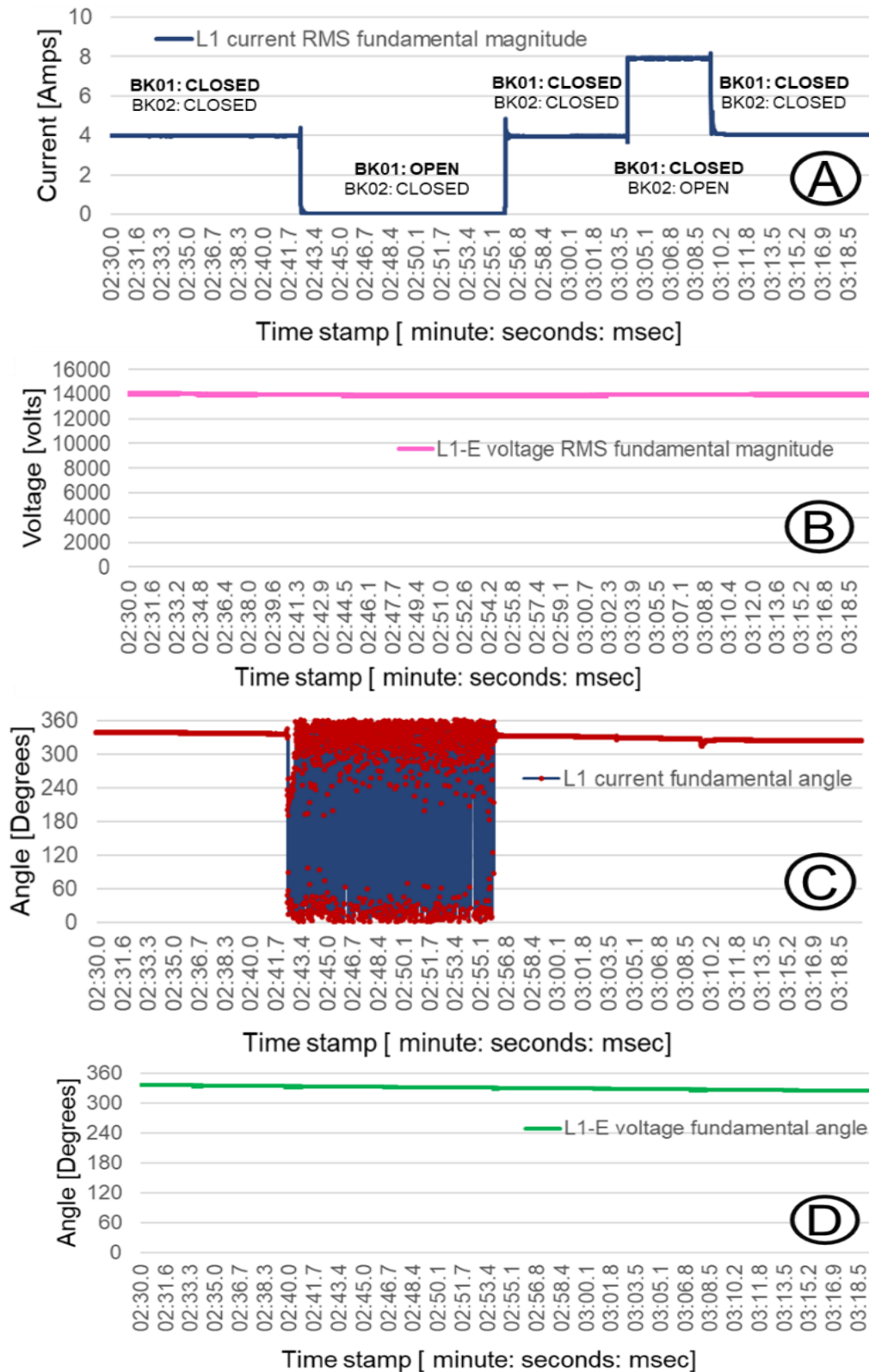


Figure 27: L1 current RMS fundamental magnitude (A) and angle (C), and L1-E voltage RMS fundamental magnitude (B) and angle (D) from the “ORNL_PMU01” micro PMU

The fundamental apparent (VA), true (W) and reactive (VAR) total power were plotted in Figure 28-A. The VA , W and VAR total power were zero when the “BK01” was opened, because no current was available. The fundamental total displacement power factor (dPF) was plotted in Figure 28-B, and it was estimated by the ratio between the measured W and VA total power.

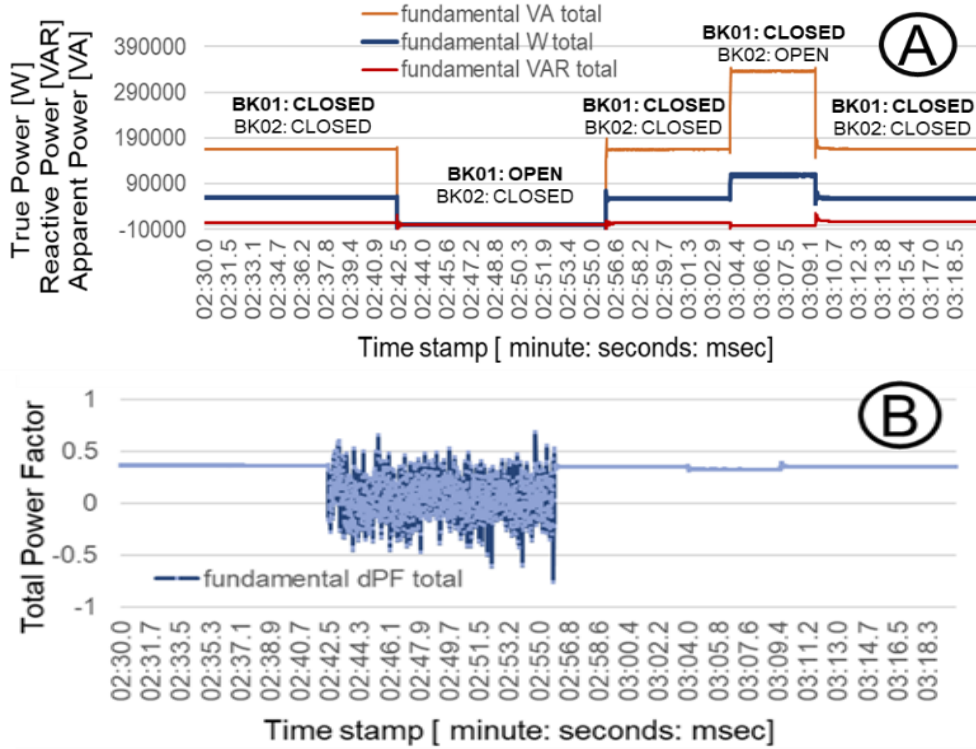


Figure 28: Fundamental apparent, true and reactive total power (A), total displacement power factor (B) from the “ORNL_PMU01” micro PMU

The dPF had a disturbance (Figure 28-B), because the W and VA total power had a noise (Figures 28-A and B) when the “BK01” breaker was opened, and no current was available. The dPF measured by the “ORNL_PMU01” micro PMU had a disturbance that was produced by the open state of “BK01” beaker. This situation should be considered when a decision based on DA is implemented using the dPF from the micro PMUs, to avoid non-desired DA estimations between electrical utilities and customers.

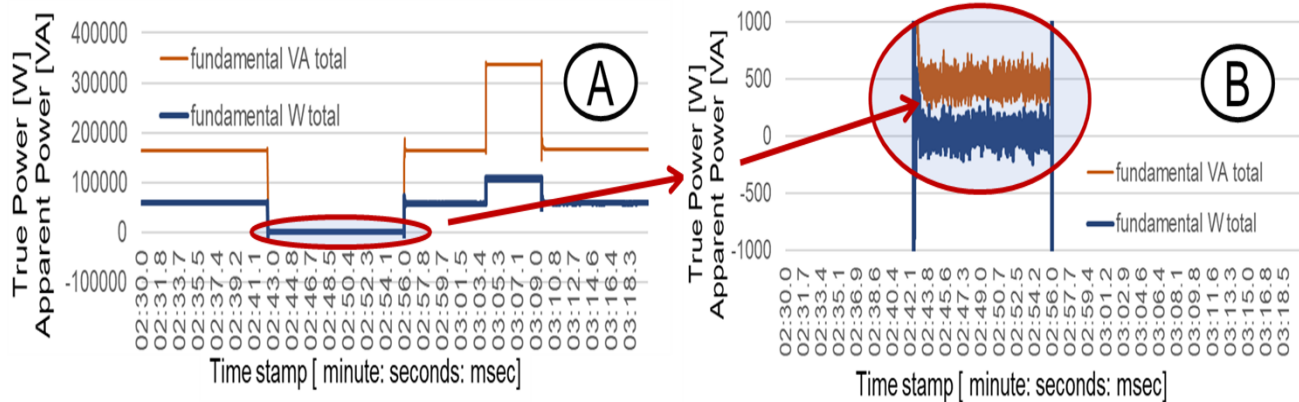


Figure 29: Fundamental apparent and, true total power (A), and zoom in total displacement power factor (B) from the “ORNL_PMU01” micro PMU

The “ORNL_PMU01” micro PMU measured the C37 L1-E and one-second L1-E frequencies are shown in Figure 30. These frequencies were based on measuring the Line 1 voltage (L1-E) frequency based on C37 protocol and the average frequency at one-second period.

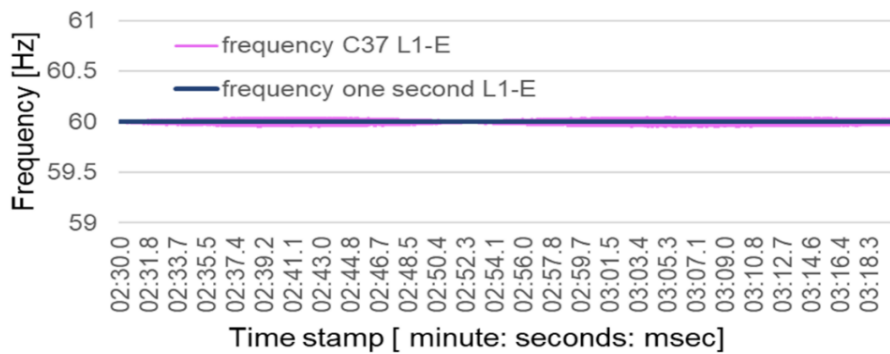


Figure 30: C37 and one-second Frequency from the “ORNL_PMU01” micro PMU

5.1.2 Data from the “ORNL_PMU02” micro PMU

In the breaker operation test, the data from the “ORNL_PMU02” micro PMU were also collected. The “ORNL_PMU02” micro PMU measured the currents and voltages of the bus at the end of the parallel power lines. The fundamental L1 current and L1-E voltage magnitudes were plotted in Figure 31-A and B, respectively. The fundamental L1 current magnitude was always eight amperes, because the parallel power lines feed the controllable resistive load bank with one or two power lines, when the “BK01” and “BK02” breakers were operated by the SACADA system.

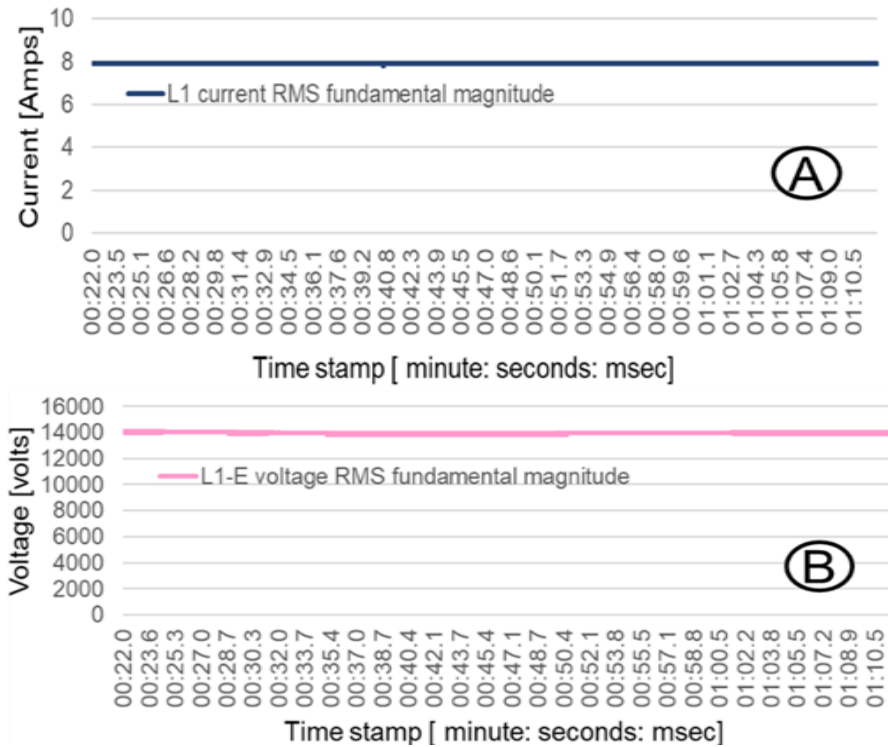
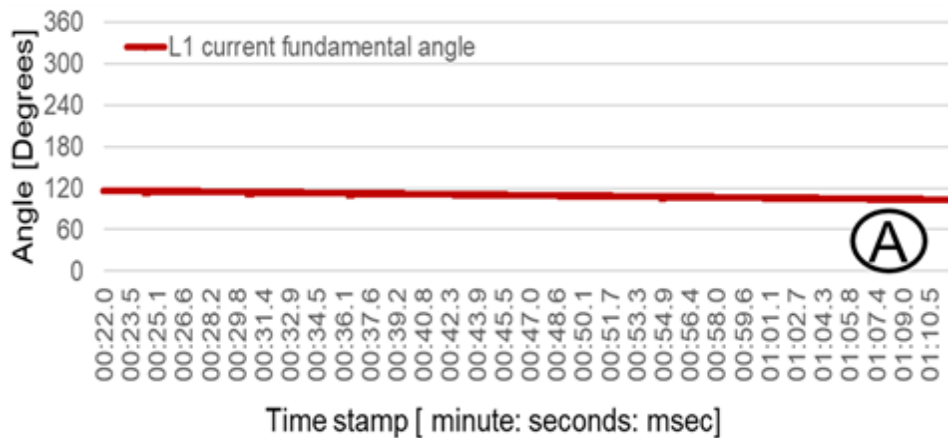


Figure 31: L1 current RMS fundamental magnitude (A) and angle (B) from the “ORNL_PMU02” micro PMU

The fundamental L1 current and L1-E voltage angles are plotted in Figure 32-A and B, respectively. The fundamental L1 current and fundamental L1-E voltage angles were measured at the end of parallel power lines. The current angle at the end of power parallel lines did not show an oscillation because no breakers were installed at the end of the parallel power lines like a radial distribution power system.



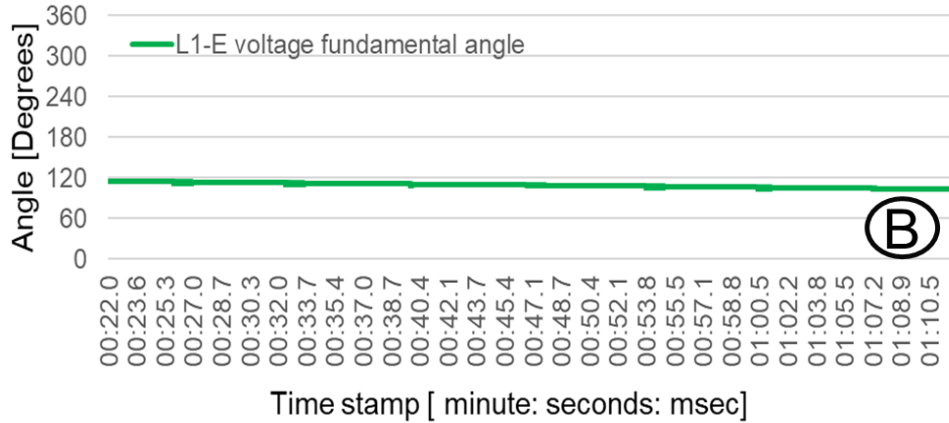
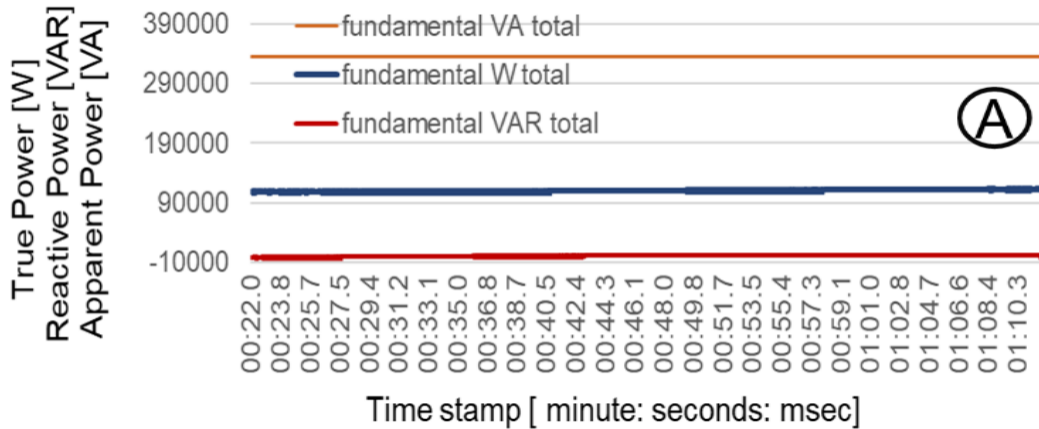


Figure 32: L1 current (A) and L1-E voltage (B) fundamental angles from the “ORNL_PMU02” micro PMU

The fundamental VA, W and VAR total power were plotted in Figure 33-A. The VA, W and VAR total power were measured at the end of the parallel power line. The *dPF* was plotted in Figure 33-B, and it was estimated by the ratio between the measured *W* and *VA* total power. The *dPF* was measured by the “ORNL_PMU02” device, and it did not show a disturbance. The “ORNL_PMU02” micro PMU was located at the end of the parallel power line, and the “BK01” and “BK02” breakers were located at the beginning of the parallel power line like a radial power distribution system. In this case, the *dPF* collected at the end of the parallel power lines without breakers could be used to make decisions based on DA, because the open state of the “BK01” breaker did not generate a noise at the measured *dPF* values, allowing to make decisions based on DA between electrical utilities and customers by using *dPF* measurements.



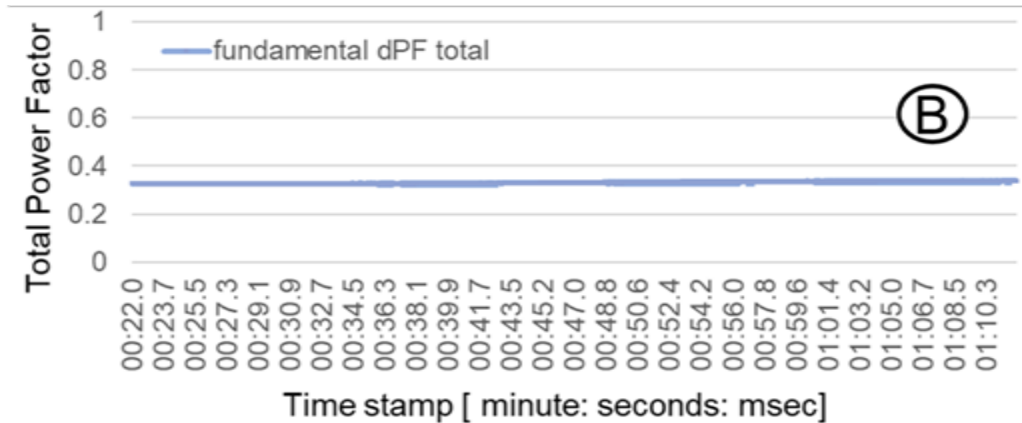


Figure 33: Fundamental apparent, true and reactive total power (A), and total displacement power factor (B) from the “ORNL_PMU02” micro PMU

The “ORNL_PMU02” micro PMU measured the C37 L1-E and one-second L1-E frequencies are shown in Figure 34. These frequencies were based on measuring the Line 1 voltage (L1-E) frequency based on C37 protocol and the average frequency at one-second period.

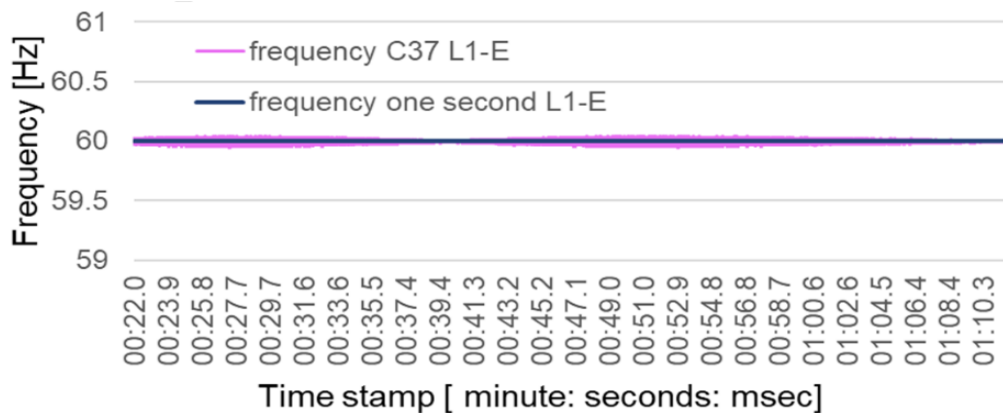


Figure 34: C37 and one-second Frequency from the “ORNL_PMU02” micro PMU

6. DISCUSSIONS

6.1 SAMPLE RATE & DATA ANALYTICS

The DA is an important tool to make decisions and improve the control and operation between electrical utilities and their residential, industrial, government and transportation customers [11]. Today’s electrical utilities estimate the DA by collecting voltages and currents from measurement devices like relays and PMUs [23]. However, electrical utilities have measurement devices from different vendors with different sample rates that could affect the collected data depending on the harmonic components at the voltage and current 60 Hz signals.

The sample rate is how fast samples are taken by the data acquisition units of measurement devices. The sample rate is measured in “samples per second”, and it is usually expressed in kilohertz (kHz), that means a collection of 1,000 data points per second. In relays and PMUs, the data acquisition unit is the

basic building block that collect the data points with a stamped time. In these devices, the data acquisition unit computes the voltage and current phasors from analog voltage and current waveforms. The operating principle of the data acquisition unit depends on the Nyquist theory [23]. As per Nyquist theorem, the analog-to-digital converter (ADC) sample rate should be greater than, or equal to, twice the signal bandwidth [23]. The sample rate (SR) of a device and can be calculated by (5)

$$SR = N_{samples\ per\ cycle} \times S_{frequency} \quad (5)$$

where $N_{samples\ per\ cycle}$ are the number of samples per cycles collected by the data acquisition unit, and $S_{frequency}$ is the signal frequency of the voltages or currents measured by the data acquisition unit in Hz.

The power system signals, like voltages and currents, are not band-limited in nature. As a result, relays and PMUs use an anti-aliasing filter to band-limit the voltage and current signals. The anti-aliasing filters are needed to avoid the situation of the sub-Nyquist sample [23]. The choice of ADC sample rate depends on the design of the anti-aliasing filter. In normal operation of power systems (oscillating at 60 Hz), measurement devices do not require a high sample rate, because voltages and currents depend on the fundamental sine wave. On the other hand, the phase-to-ground faults in transmission lines could create harmonics at transient states that are originated by the capacitance added along the transmission line. Then, currents and voltages could be superimposed on the fundamental frequency component due to the capacitance of the transmission line [24]. In addition, the switching frequency of DC/DC and DC/AC converters, operate with the Pulse Width Modulation (PWM) technique, and is higher than 3 kHz [25]. Hence, higher order harmonics up to the 100th order could be generated in large scale photovoltaic systems where converters with voltage notching, high pulse numbers, or PWM controls result in induced current distortions [26].

The study of power systems at normal (oscillating at 60 Hz) and non-normal (disturbances with harmonics components) operations require low and high sample rates, respectively, to estimate the DA from measurement devices (relays, PMUs and micro PMUs). Currently, commercial relays use sample rates ranging from 8 to 96 samples per cycle [23]. On the other hand, PMUs use sample rates ranging from 30 to 120 samples per cycle [27]. The PMU can measure 60 Hz AC waveforms (voltages and currents) typically at a rate of 48 samples per cycle [28]. However, the micro PMUs use sample rate (phasor measurement per seconds) ranging from 10 to 120 samples per cycle, as it is shown at the micro PMU setting screen in Figure 35.

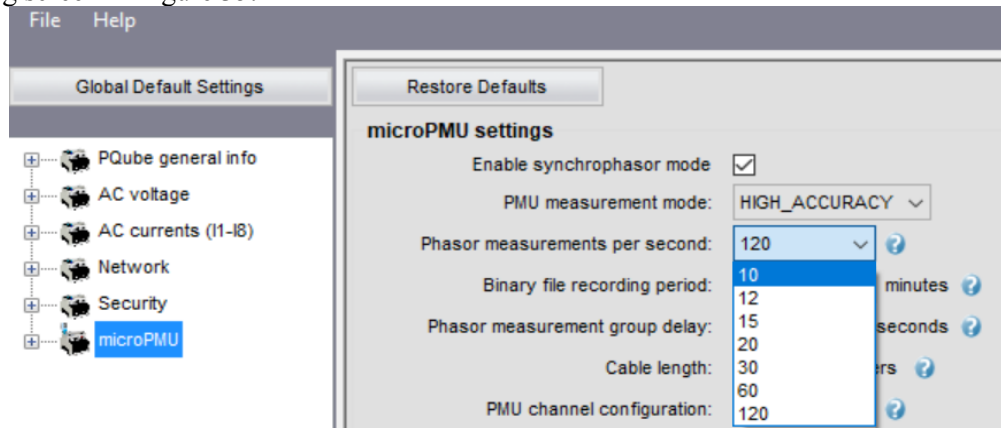


Figure 35: Setting screen of sample rate for the micro PMU

From Equation (5), the curves for PMUs (120 and 30 samples per cycle), relays (96 and 80 samples per cycle), and micro PMUs (2 and 0.167 samples per cycle) for maximum and minimum sample rates are

shown in Figure 36. The PMU, Relay, and micro PMU curves were plotted in green, blue and red. The solid and dash lines represent the maximum and minimum sample rating curves, respectively. While the micro PMU can measure the fundamental currents and voltages, the PMUs and Relays can measure the harmonics of 60 Hz fundamental sine wave for currents and voltages.

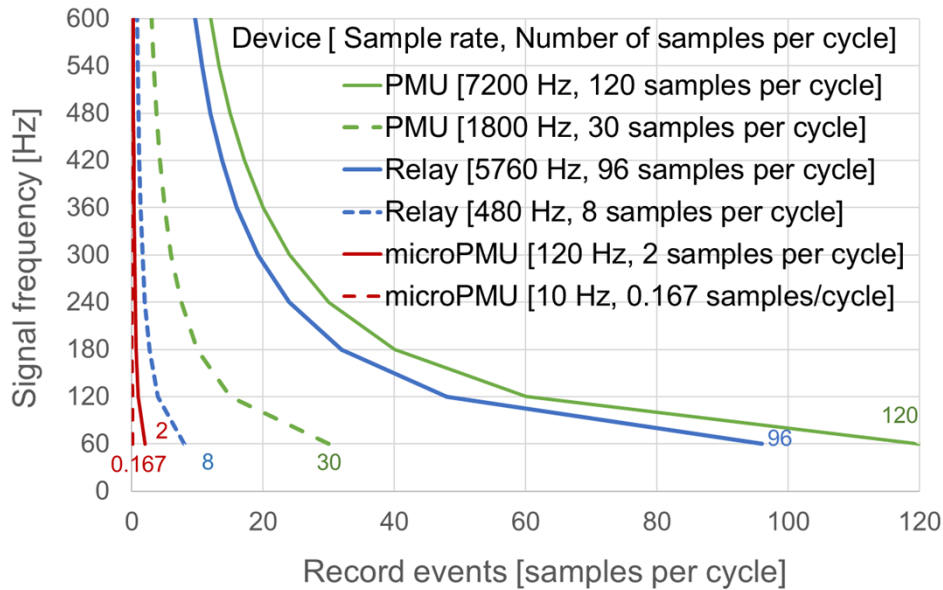


Figure 36: Sample rate curves for PMU, Relay, and micro PMU

The Nyquist frequency for sample rate curves represents the limit of the signal frequency to be measured by the devices (PMU, Relay, and micro PMU). The Nyquist frequency is a type of sampling frequency that is defined as “half of the rate” of a discrete signal processing system [23]. Then, the Nyquist frequency for the maximum sample rate curves of PMUs, Relays, and micro PMUs can be estimated. Figure 37 shows the estimated Nyquist frequency for the PMUs, Relays and micro PMUs. Based on the Nyquist theory, the maximum available signal frequencies for the PMUs, Relays and micro PMUs are 3600, 2880, and 60 Hz, respectively.

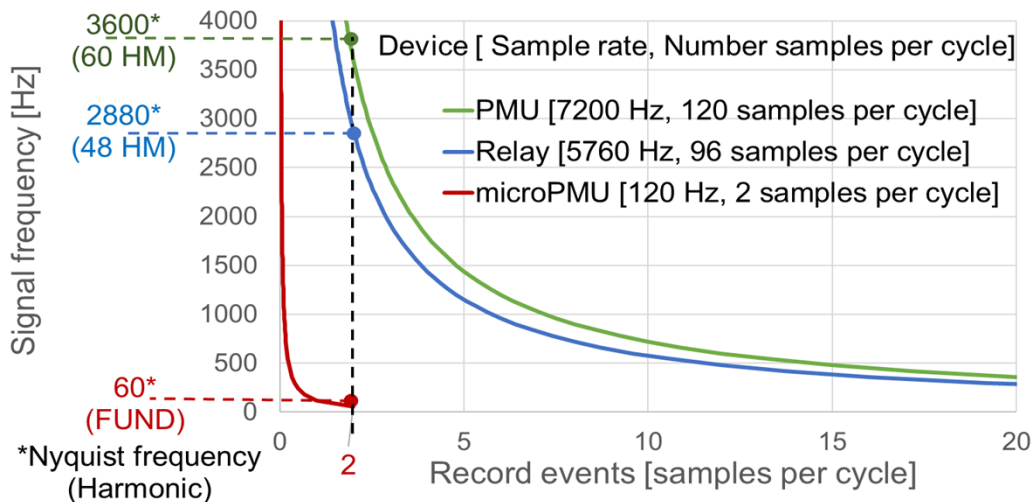


Figure 37: Nyquist frequency for PMU, Relay, and micro PMU

Measurement devices like PMUs, relays and micro PMUs should be selected to collect data that allow a good DA estimation, based on sample rates that allow to measure the fundamental and harmonics of current and voltage signals. From Figure 37, commercial PMUs and Relays could measure voltage and current signals of 60 and 48 harmonics, respectively. Then, using PMUs and Relays could allow to estimate the DA for normal operation (oscillating at 60 Hz), and harmonics disturbances in power systems. However, micro PMUs could only be used for normal operation (oscillating at 60 Hz) in power systems.

6.2 DATA ANALYTICS MAP FOR BREAKER OPERATION TESTS WITH MICRO PMUS

The map of DA for the breaker operation tests with the micro PMUs was presented in Table 6. The breaker operation tests allowed to collect the estimated fundamental voltages, currents, frequency, and total true, reactive and apparent power, and displacement power factor from the micro PMUs. The fundamental total displacement power factor, and real and apparent total power had a noise when the “BK01” breaker was opened. This map indicates the available DA applications for the “ORNL_PMU01” and “ORNL_PMU02” micro PMUs, based on the “BK01” and “BK02” breaker states. The DA application and decisions for the electrical utility and customers (residential, industrial, commercial and government) could be validated by collecting the estimated fundamental voltages, frequency, and total true, reactive and apparent power, and displacement power factor from the micro PMUs.

In Table 6, the DA applications based on the electrical energy (kWh , $kVARh$) and electrical energy consumption ($kWh/month$, kWh/day) were not directly estimated by the micro PMUs. Then, the electrical energy and energy consumption could be estimated using the stamped time measured by the micro PMUs. The micro PMUs could also estimate the On-peak times also known as the on-peak hours that are when the electricity demand is the highest, and customers could pay the highest amount per kWh . In the summer, these hours are typically from 10:00 am- 8:00 pm during weekdays. In the winter, these peak hours are typically around 7:00 am to 11:00 am and 5:00 am to 9:00 pm.

Table 6: Map of available data analytics for breaker operation tests with micro PMUs

Test	States of “BK01” Breaker ^[1]	CLOSED		OPEN		CLOSED		CLOSED		CLOSED		
	States of “BK02” Breaker ^[2]	CLOSED		CLOSED		CLOSED		OPEN		CLOSED		
	micro PMU ORNL_	PMU01	PMU02	PMU01	PMU02	PMU01	PMU02	PMU01	PMU02	PMU01	PMU02	
Micro PMU Data	L1, L2, L3 E voltage RMS fundamental magnitude	B3-C3	B3-C3	B3-C3	B3-C3	B3-C3	B3-C3	B3-C3	B3-C3	B3-C3	B3-C3	
	Fundamental real total power	A1*-A2* A3-A4 B1*-B2* B4* C1*-C2*	A1*-A2* A3-A4 B1*-B2* B4* C1*-C2*	NOISE	A1*-A2* A3-A4 B1*-B2* B4* C1*-C2*	A1*-A2* A3-A4 B1*-B2* B4* C1*-C2*	A1*-A2* A3-A4 B1*-B2* B4* C1*-C2*	A1*-A2* A3-A4 B1*-B2* B4* C1*-C2*	A1*-A2* A3-A4 B1*-B2* B4* C1*-C2*	A1*-A2* A3-A4 B1*-B2* B4* C1*-C2*	A1*-A2* A3-A4 B1*-B2* B4* C1*-C2*	A1*-A2* A3-A4 B1*-B2* B4* C1*-C2*
	Fundamental reactive total power	A1*-A2* A4	A1*-A2* A4	A1*-A2* A4	A1*-A2* A4	A1*-A2* A4	A1*-A2* A4	A1*-A2* A4	A1*-A2* A4	A1*-A2* A4	A1*-A2* A4	A1*-A2* A4
	Fund. total displacement power factor	A1-A2- C4	A1-A2- C4	NOISE	A1-A2- C4	A1-A2- C4	A1-A2- C4	A1-A2- C4	A1-A2- C4	A1-A2- C4	A1-A2- C4	A1-A2- C4
	C37 L1-E frequency	A4-B3- C3	A4-B3- C3	A4-B3- C3	A4-B3- C3	A4-B3- C3	A4-B3- C3	A4-B3- C3	A4-B3- C3	A4-B3- C3	A4-B3- C3	A4-B3- C3
Data Analytics	A-Electrical Utility’s Decision [Data]	B-Residential Customer’s Decision [Data]				C-Industrial, Commercial & Government Customer’s Decision [Data]						
	A1 -To monitor real-time customer consumptions [<i>kWh, kVARh, power factor</i>]	B1 -To modify customer electricity usage habit to save money [<i>kWh/ month</i>]				C1 -To create efficiency programs to reduce environmental impact, reducing CO2 emission [<i>kWh/ month</i>]						
	A2 -To offer new real-time tariff models based on customer usage habits with rewards/punishments [<i>kWh, kVARh, power factor</i>]	B2 -To make accurate and timely decisions for electrical billing [<i>kWh/ day</i>]				C2 -To improve the load forecasting for industrial and/or commercial activities [<i>kWh/day</i>]						
	A3 -To improve the load management for the power lines [<i>Line power losses</i>]	B3 -To supervise energy quality provided by the utility to avoid damage to electrical appliances [<i>Voltage and Frequency</i>]				C3 -To supervise energy quality provided by the utility to avoid damage to electrical industrial equipment [<i>Voltage and Frequency</i>]						
A4 -To control energy and grid resources efficiently [<i>Voltage, Frequency, Active Power, Reactive Power</i>]	B4 -To operate electrical equipment during hours with less expensive fees [<i>On-peak times</i>]				C4 -To install capacitor banks to avoid utility’s bill penalties [<i>Power factor</i>]							

^[1] “BK01” Breaker is located at beginning of parallel power line, ^[2] “BK02” Breaker is located at end of parallel power line, *Micro PMU data require to collect also the time (yy, mm,dd, hh,min) to calculate the final data.

Based on Table 6, electrical utilities could monitor their customer consumptions by measuring the electrical energy in real-time, to offer new real-time tariff models based on customer usage habits focused on reward and punishment options. Electrical utilities could improve the load management by measuring the line power losses with micro PMUs located at the beginning and end of power lines, and also control the energy and grid renewable resources efficiently by measuring the voltage, frequency, active and reactive power along the power system. Residential customers could modify their electricity usage habits to save money, and make accurate and timely decisions that impact electrical billing.

House owners could supervise the energy quality provided by the utility to avoid damage to electrical appliances by measuring voltage and frequency. In addition, residential customers could avoid using electrical equipment during hours with higher fees due to peak consumption, and switch electrical equipment on during hours with less expensive fees. On the other side, Industrial, Commercial & Government Customers could create efficiency programs to improve the environmental impact based on reducing CO2 emission, and improve the load forecasting for industrial and/or commercial activities. Big customers could supervise the energy quality provided by the electrical utility to avoid damage to electrical industrial equipment, measuring voltage and frequency levels, and also make decisions about installing capacitor banks to avoid utility's bill penalties by low power factor penalties.

6.3 COMPARISON OF OPENFMB AND LBNL STREAM-PROCESSING ARCHITECTURE FOR REAL-TIME CYBERPHYSICAL SECURITY (SPARCS)

Open Field Message Bus (OpenFMB) is a reference architecture and framework for distributed intelligence and grid-edge interoperability that leverages existing standards to federate data between field devices and harmonize them with centralized systems. It uses utility industry standardized semantic models such as the IEC's Common Information Model (CIM), used in first reference implementation, and the IEEE 61850, with which it is in the process of harmonizing with CIM for the current implementation.

LBNL SPARCS is a stream-processing architecture for real-time data analysis focused mainly on cybersecurity applications. It is currently built to read from micro PMUs and send data out to RabbitMQ and Cassandra in its' reference implementation. Following is a table that breaks down and compares the features of OpenFMB and LBNL's SPARCS.

Table 7: Comparison of SPARCS and OpenFMB

Feature	OpenFMB	LBNL SPARCS
<i>Intent</i>	Architecture and framework for distributed intelligence and grid-edge interoperability	Purpose built for real-time cyber-physical security applications
<i>Purpose</i>	Not specific for cybersecurity	Stream-processing architecture for real-time data cyber-physical security analysis
<i>Protocol</i>	Uses protocol translators	Could potentially but designed mainly for high-speed protocols
<i>Implementation</i>	Can be implemented on devices natively in the future	Built to be run as a standalone
<i>Data input</i>	Through a protocol translator such as an RTAC at a potentially slower rate	Reads from PMUs using C37.118
<i>Network communication paradigm</i>	It can be implemented without restriction currently NATS	Currently implemented on RabbitMQ

Data output	No restriction, can push data on backend OpenFMB app to any format, currently implemented in python to write out to csv	Can push data to Splunk and OSISoft-Pisystem
	Data model profiles built for interacting with many different grid devices	Mainly for mPMUs

Table 7 shows a side-by-side comparison of the features for OpenFMB and LBNL SPARCS framework. Built for slightly different purposes of enabling better data analytics in OpenFMB and SPARCS focusing on cybersecurity applications of data analytics, their approach to analytics is different. OpenFMB is a data model while SPARCS in a full architecture. In theory SPARCS could use OpenFMB’s data model.

7. CONCLUSIONS

The study of power system events using DA is crucial to improve the control and operation between electrical utilities and their customers (residential, industrial, transportation, commercial and government). Measurement devices like PMUs, relays and micro PMUs should be selected to collect data that allow the DA estimation based on sample rates, to measure the fundamental and harmonics of current and voltage signals. The PMUs and Relays could measure voltage and current signals of 60 and 48 harmonics, respectively. Then, using PMUs and Relays could allow to estimate the DA for normal operation (oscillating at 60 Hz), and harmonics disturbances in power systems. However, micro PMUs could be used for only normal operation (oscillating at 60 Hz) in power systems.

Comparing the breaker operation experiments collected voltages, currents, frequency, and total true, reactive and apparent power, and displacement power factor from the micro PMUs with the data obtained through network traffic collection and OpenFMB we observed that we can have a more varied view of our system using OpenFMB with recommended custom network traffic fields. In addition, the breaker operation test shows that the fundamental L1 current angle measured by the “ORNL_PMU01” micro PMU had a noise that was produced by the open state of “BK01” breaker. Also, the fundamental dPF (estimated by the ratio between the measured W and VA total power) had a disturbance, because the W and VA total power had a noise when the “BK01” breaker was opened, and no current was available. These situations should be considered when a decision based on DA is implemented using the L1 current angle and dPF from the micro PMUs, to avoid non-desired DA estimations between electrical utilities and customers.

Machine learning applications can leverage the OpenFMB data model to share raw sensor data to any devices that subscribe. Analytics can be calculated on nodes to identify attributes that can be used for preventative maintenance and attack detection. Features traditionally used for network forensics can be incorporated into a new OpenFMB data model and shared for security analytics. We see that behaviors for DoS attacks differ from hardware LAN cable problems. Ping floods, SYN floods and UDP floods all have a slightly different effect. By calculating network metrics and combining with sensor data we can have a better view of the system and validate observed events with the redundant data sources.

While LBNL’s SPARCS framework has functionality that is similar to OpenFMB in certain contexts they are essentially built for distinct purposes. They can complement each other and be used side-by-side together or combined with some modifications to SPARCS. OpenFMB is meant to be a universal language for grid devices and eventually for all CPS systems through custom-made profiles for all industrial control systems while SPARCS is a framework specifically built for cybersecurity analytics to

use with micro PMU data. The advantage of combining both OpenFMB and SPARCS is the added universality of using a common data model for analytics. This can join features from sensors, synchrophasors and network devices like switches or firewalls.

This report describes how electrical utilities, residential, industrial, and commercial and government customers can use grid edge devices to make decisions using DA applications. Electrical utilities use DA applications to monitor real-time customer consumptions, offer new real-time tariff models based on customer usage habits (rewards and punishments), provide energy peak during peak load times (plan energy generation and distribution), improve the transformer load management for the power lines, control energy and grid resources efficiently, and define actual grid modes and possible grid operations. The residential customers use DA applications to modify customer electricity usage habit to save money, make accurate and timely decisions for electrical billing, supervise energy quality provided by utility to avoid damage electrical appliances, switch electrical equipment off during expensive hours with significant consumption, and on during less expensive hours, and to program home tasks and turn off sensitive electrical equipment.

REFERENCES

[1] Y. Zhang, T. Huang, and E. F. Bompard, "Big data analytics in smart grids: a review," *Energy Informatics*, 2018 1:8, pp. 1-24, available: <https://doi.org/10.1186/s42162-018-0007-5>

- [2] M. Milby, H. Keegan and J. Will Bake, “Intelligent Efficiency and Utility Programs Reports from the Midwest,” Midwest Energy Efficiency Alliance, February 2017, pp. 1-31
- [3] J. Zhu, E. Zhuang, J. Fu, J. Baranowski, A. Ford, “A Framework-Based Approach to Utility Big Data Analytics,” IEEE Transactions on Power Systems, vol. 31, no. 3, pp. 2455-2462.
- [4] A. Abur and A. G. Exposito, Power system state estimation: theory and implementation. CRC press, 2004.
- [5] M. Jamei, A. Scaglione, C. Roberts, E. Stewart, S. Peisert, C. McParland, A. McEachern, “Anomaly Detection Using Optimally-Placed μ PMU Sensors in Distribution Grids,” IEEE Transactions on Power Systems, 2017, pp. 1-12
- [6] M. Kezunovic, L. Xie, and S. Grijalva, “The role of big data in improving power system operation and protection,” in 2013 IREP Symposium Bulk Power System Dynamics and Control - IX Optimization, Security and Control of the Emerging Power Grid, Aug 2013, pp. 1–9.
- [7] A. Phadke and R. M. de Moraes, “The wide world of wide-area measurement,” Power and Energy Magazine, IEEE, vol. 6, no. 5, pp. 52–65, 2008.
- [8] V. Terzija, G. Valverde, D. Cai, P. Regulski, V. Madani, J. Fitch, S. Skok, M. M. Begovic, and A. Phadke, “Wide-area monitoring, protection, and control of future electric power networks,” Proceedings of the IEEE, vol. 99, no. 1, pp. 80–93, 2011.
- [9] J. H. Eto, E. M. Stewart, T. Smith, M. Buckner, H. Kirkham, F. Tuffner, and D. Schoenwald, “Scoping study on research and priorities for distribution-system phasor measurement units,” 2015.
- [10] “Standards and Interoperability in Electric Distribution Systems,” Office of Energy Policy and Systems Analysis, ICF, VA, USA, US Department of Energy, October 5, 2016, pp. 1-78.
- [11] “Energy and the Environment - Electricity customers,” United States Environmental Protection Agency. Available on 6/6/19: <https://www.epa.gov/energy/electricity-customers>
- [12] “Save Time and Resources with the NI CompactRIO General Purpose Inverter Controller (GPIC),” National Instruments, Available on 6/6/19: <https://www.ni.com/en-us/innovations/white-papers/12/save-time-and-resources-with-the-ni-compactrio-generalpurpose-i.html>
- [13] “OpenFMB™-CollaborationSite,” Available on 6/6/19: <https://github.com/openfmb>
- [14] D. Merkel, “Docker: Lightweight Linux containers for consistent development and deployment,” Linux Journal, May 19, 2014, Available on 6/6/19: <https://www.linuxjournal.com/content/docker-lightweight-linux-containersconsistent-development-and-deployment>
- [15] M. H. Cintuglu, O. A. Mohammed, K. Akkaya, and A. S. Uluagac, “A Survey on Smart Grid Cyber-Physical System Testbeds,” IEEE Communications Surveys & Tutotrials, vol. 19, no. 1, first quarter 2017, pp. 446-464.
- [16] “microPMU Installation and User Manual,” Revision 2.0, Power Sensors Ltd., 980 Atlantic Ave, Alameda, CA, USA. 2008-2016, pp. 1-53, Available online 6/6/19: www.PowerSensorsLtd.com

- [17] “MicroPMU Quickstart Kit Administration guide for adding, removing, and managing MicroPMU data, MicroPMU Quickstart Kit Administrator Manual,” Revision 17, Power Sensors Ltd., 980 Atlantic Ave, Alameda, CA, USA. 2008-2016, pp. 1-65, Available online 6/6/19: www.PowerSensorsLtd.com
- [18] microPMU Configurator® 3.6.0.3 software.
Available on 6/16/19: <https://www.powerstandards.com/download-center/micropmu/?file=5654>
- [19] PMU Connection Tester® v4.5.11 software.
Available on 6/16/19: <https://github.com/GridProtectionAlliance/PMUConnectionTester/releases>
- [20] Open PDC® v2.6 software.
Available on 6/16/19: <https://github.com/GridProtectionAlliance/openPDC/releases>
- [21] FileZilla Client® software. Available on 6/16/19: <https://filezilla-project.org/>
- [22] MicroPMU File Converter® software.
Available on 6/16/19: <https://www.powerstandards.com/download-center/micropmu/#4>
- [23] S. Das, “Sub Nyquist Rate ADC Sampling in Digital Relays and PMUs Advantages and Challenges,” 2016 IEEE 6th International Conference on Power Systems, New Delhi, India, 4-6 March 2016, pp. 1-6.
- [24] T. Kase, Y. Kurosawa and H.Amo, “Charging Current Compensation for Distance Protection,” IEEE Transactions on Power Delivery, vol. 23, no 1, Jan. 2008, pp. 124-131.
- [25] M. García-Gracia, N. El Halabi, A. Alonso and M. Paz Comech, “Harmonic Distortion in Renewable Energy Systems: Capacitive Couplings, Open access peer-reviewed chapter, Chapter 11, 2011, 261-278, DOI: 10.5772/17677
- [26] G. Chicco, J. Schlabbach, F. Spertino, “Experimental assessment of the waveform distortion in grid connected photovoltaic installations,” Solar Energy Journal, Elsevier, vol. 83, no 7, July 2009, pp. 1026-1039.
- [27] R. B. Bobba, J. Dagle, E. Heine, H. Khurana, W. H. Sanders, P. Sauer, and T. Yardley, “Enhancing Grid Measurements,” IEEE Power & Energy Magazine, January/February 2012, pp. 67-73.
- [28] C. Mishra, D.K. Mohanta, “Modelling of Phasor Measurement Unit and Phasor Data Realisation with 2 Bus System,” International Journal of Advanced Engineering Science and Technological Research, 2015 June, pp. 1-6.
- [29] M. Chen, S. Mao, Y. Liu, “Big data: a survey”, Mob. Netw. Appl. 19 (2) (2014) 1–39.[30] Sonal Patel. <https://www.powermag.com/new-approaches-for-transformer-operation-and-maintenance-2/>,
- [31] Akhavan-Hejazi H, Mohsenian-Rad H. Power systems big data analytics: An assessment of paradigm shift barriers and prospects. Energy Reports 2018;4:91–100. doi:10.1016/j.egy.2017.11.002.
- [32] UDP Flood, <https://www.imperva.com/learn/application-security/udp-flood/>, accessed 08/19
- [33] Holtz M D, David B M, de Sousa Júnior R T. Building Scalable Distributed Intrusion Detection Systems Based on the MapReduce Framework[J]. REVISTA Telecomunicacoes, 2011 (2): 22-31.

[34] B. Ollis, P. Irringer, M. Buckner, I. Ray, D. King, A. Herron, B. Xiao, R. Borges, M. Starke, Y. Xue, and B. Maccleery, "Softwaredefined intelligent grid research integration and development platform," in IEEE Power Energy Society Innovative Smart Grid Technologies Conference (ISGT), Sept 2016, pp. 1–5.